National University of Lesotho

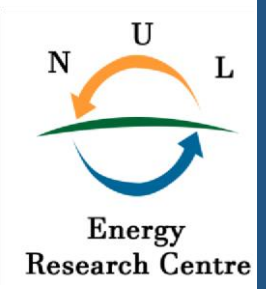

Optimal sizing, performance prediction and economic appraisal of off-Grid Solar PV hybrid power systems in Lesotho: A reliability –cost approach

Selone Augustinus Lepolesa 201804353

A dissertation submitted in partial fulfilment of
the requirements for the degree of

Master of Science in Sustainable Energy

Offered by the

Energy Research Centre
Faculty of Science & Technology

February 2020

Abstract

This dissertation reports about the development of and the application of a simple spreadsheet-based mathematical model for the sizing, the performance prediction, and the economic analysis of a PV-Diesel-Battery autonomous power supply system. The main objective was to find appropriate reliability level required of a mini-grid system in Lesotho that minimized the Levelized Cost of Energy (LCOE), and at the same time, supplied a satisfactory energy service. The goal was to determine the costeffective level to set for the energy reliability for mini-grids in Lesotho, such that the LCOE would not increase disproportionately with the marginal increase in the reliability level. The method used was to find the reliability at the minimum cost using the elbow of the graph. The simulation and performance analysis showed that there was an infinite number of combinations of battery, PV array and diesel generator size required to achieve a given supply reliability. It was observed that the conditions for minimum LCOE may not correspond to highest reliability and satisfactory energy service.

Acknowledgements

I would like to express my very great appreciation to Engineer T. Hove for his valuable and constructive suggestions during the planning and development of this research work. His willingness to give his time so generously has been very much appreciated.

Contents

List of Tables

List of Figures

Chapter 1: Introduction and Background

1.1 Introduction

According to Lewandowska-Bernat and Desideri, more than 1.5 billion people worldwide did not have access to electricity in their homes , which problem was called “power poverty” [1]. Sub-Saharan Africa (SSA) had the lowest electrification rate globally, as, only 31 % of the population had access to modern energy services [2]. In Lesotho, according to SE4ALL [3], only 16% of the rural population had access to electricity services, since the extension of the national grid to remote rural areas was prohibitively expensive [4], [5]. Lesotho depended on the use of imported fossil fuels to satisfy its energy requirements even though the country had good renewable energy resources (e.g. solar power, hydropower, and wind power) [6].

The opportunity to provide clean electricity in regions where modern electrical services were not available yet could offer a considerable chance to also advance the employment of sustainable energy resources [7]. The provision of electricity via distributed renewable energy systems had the potential of eradicating poverty, providing clean and affordable energy to all, and of taking action to reduce climate change directly [8].

The share of the total power generation provided by renewables was increasing rapidly in the developed and developing countries, and many countries aimed to change and improve the composition of their energy sectors towards the inclusion of the renewables [9]. Hence, among other developmental activities Lesotho also identified 30 potential renewable-based mini-grid sites in 2014 through the 2001 Access Study, the 2007 National Electrification Master Plan (NEMP), and the 2016 United Nations Development Programme (UNDP) Sustainable Energy For All (SEforALL) projects [6]. It should be noted, however, that mini-grids had previously already been functioning in Lesotho: mini-grids were operational between 1983 and 1993 in places such as Semonkong (300 kW), Tlokoeng (670 kW), Mantśonyane (2 MW) and Tsoelike (400 kW) [5], but only the Semonkong mini-grid was still operational at the time of this study.

Endeavoring seriously to reduce GHG emissions and to contribute to the achievement of Lesotho's Vision 2020 and SE4All goals, the Government of Lesotho called for relevant Investment Proposals. The Government, through the Ministry of Energy and Meteorology (MEM) and United Nations Development Programme (UNDP), called for Investment Proposals as part of the implementation of the "Development of Cornerstone Public Policies and Institutional Capacities to Accelerate Sustainable Energy for All (SE4All) Progress" Project. The program focussed on establishing renewable energy mini-grids with at least 18 kW of PV at ten pre-identified villages: Ketane (Ha Nohana) and Ribaneng in Mohale's Hoek; Matsoaing and Tlhanyaku in Mokhotlong; Sehlabathebe (Mpharane) and Lebakeng in Qacha's Nek; Tosing (Dalewe) and Sebapala (Ha Sempe/Lefikeng) in Quthing, Sehonghong and Mashai (Moreneng, St. Theresa) in Thaba-Tseka [10]. Lesotho was also developing a regulatory framework for the development of local renewable energy resources following the examples of other Sub-Sahara African countries [11].

According to AF-Mercados EMI (2015), one of the objectives of the regulatory framework was "the development of the principles underlying the determination of tariffs for Renewable Energy Sources Electricity (RES-E) appropriate to attract investments in RES-E, based on a comprehensive economic and financial model that would integrate cost structures, technical characteristics, economic, financial and financing parameters, to provide a basis for assessing the costs and tariffs of various RES-E technologies, pricing, and for the facilitation of negotiations of PPAs". Therefore, the optimal sizing, the performance prediction, and the economic appraisal of an off-Grid Solar PV hybrid power system were deemed to be substantial in determining the cost of off-grid solar PV power systems.

Another important consideration regarding the sustainability of the mini-grid system was the clarification of the level of supply reliability that the power systems would be operated at, bearing in mind that an increase in reliability involved a disproportionate increase in the cost of energy. A reliability-cost approach was therefore used to determine the most cost-effective level of reliability to operate at.

1.2 Historical development and current state

Lesotho's development objectives were contained in the National Strategic Development Plan 2012/13 – 2016/17, Lesotho Energy Policy 2015-2025, and Lesotho Vision 2020. These objectives were (1) to develop a basic infrastructure to increase access to services and markets and strengthen linkages between rural and urban markets, (2) to contribute towards the improvement of the livelihoods of its citizens, and (3) to contribute towards poverty alleviation in Lesotho [5], [12]–[14]. The objectives would be achieved through the creation of income-generating opportunities that sustain and improve the lives of the people in the country by facilitating the provision of affordable technologies and services and the development of an effective economic infrastructure, that would include electricity networks and thus reduce the gap between the rich and the poor.

SSI A DHV COMPANY's consultants (2009) identified the potential sites and established the technical and economic conditions required to install solar power generation equipment based on the radiation map of Lesotho (SSI A DHV COMPANY, 2009). This radiation map identified suitable sites with high levels of radiation that were situated close to transmission lines and industrial end-users.

1.3 Research problem

At the time that this study was done, the method used in Lesotho for sizing Solar PV installations and predicting performance used a Daily Energy Balance approach which had many limitations and did not provide answers to some of the crucial questions about the sizing, the cost, and the reliability of the Solar PV systems used in minigrids. This method did not differentiate between different diurnal load profiles when sizing batteries and PV arrays. This limitation could lead to over-sizing or under-sizing of battery banks, PV arrays, the inverters and the back-up energy supplies. Oversizing would invariably lead to the designing of unnecessarily costly systems. Undersizing would invariably result in disappointing energy yields. Furthermore, the use of this approach did not allow for the flexibility of decreasing the required battery capacity as the PV array size increased. The use of the method was further restricted since it could not be used to decide on the optimal PV-battery size combination for different choices of reliability levels of the supply, as it always assumed a 100 % reliability level, and

had no way of calculating other levels of energy supply reliability. Given the situation outlined above, the research questions for this study was formulated as follows:

- What should be the appropriate reliability level required of a mini-grid system in Lesotho, that minimized the Levelised Cost of Energy (LCOE), and at the same time, supplied a satisfactory energy service?
- What should be the Levelized Cost of Energy (LCOE) for any architectural combination off-grid power system;
- What should be a method for the modeling of the hourly load profile where the historical consumption data was never measured nor recorded?

1.4 Research objectives

The aim of this study (project) was to provide a method for choosing the most costeffective reliability level to set for a mini-grid in Lesotho, based on a comprehensive review of extant relevant literature and industry practices. Particularly, the study had the following sub-objectives:

- To demonstrate the importance of considering the diurnal load profile in the sizing of (off-grid) mini-grid systems (i.e. hybrid PV-diesel-battery autonomous power supply systems);
- To perform the Sizing of an off-grid power system to achieve any desired level of energy supply reliability;
- To determine the Levelized Cost of Energy (LCOE) for any architectural combination off-grid power system;
- To develop models for *in-plane solar radiation available*, *time-step PV generator output*, *battery lifespan as a function of battery size*, *depth and rate of discharge;*
- To determine the back-up generator's specific fuel consumption and lifespan as functions of load-ratio, to enable the selection of the most suitable diesel generators;
- To determine (as a matter of great importance) the cost-effective level to set for the energy reliability for mini-grids in Lesotho, such that the LCOE would not increase disproportionately with the marginal increase in the reliability level;

- To propose a method for the modeling of the hourly load profile where the historical consumption data was never measured nor recorded.

While the objective was to minimise the LCOE, the minimum LCOE did not necessarily correspond to the reliability that was desired. Conversely, minimising LCOE was making the system so small that the desired reliability was not reached.

1.5 Rationale for the study

The rationale of this study was to find answers to inform planning and policy decisions about the technology options regarding the future role of off-grid hybrid systems in support of the National Lesotho Vision 2020, the Lesotho Energy Policy 2015-2025 and National Strategic Development Plan 2012/13-2016/17. The benefits of employing properly-sized off-grid hybrid systems were reported to include earning additional income to improve and expand the power generation, transmission and distribution infrastructure, enhancing the electricity supply, increasing the power generation for the country to meet the local demand and enhancing the security of energy and electricity supply [11].

The SSI A DHV COMPANY consultants' report, based on the radiation map of Lesotho, indicated the potential sites for the installation of solar power generation equipment and established the associated technical and economic conditions [14]. Following this work, this study also intended to add to the scientific knowledge of this field by determining the most cost-effective reliability level and the LCOE of PV offgrid hybrid systems for Lesotho. The outcomes of this research would be of benefit all the citizens and, particularly, the energy sector of the Country. The study also intended to promote the reduction of GHG emissions, thus contributing to the achievement of the goals of Lesotho's Vision 2020 and the SE4All projects. Importantly, it was the intention that the results of the study would enhance the public's appreciation of the policy considerations in the field of sustainability and would promote relevant dialogue and discourse. Lastly, it intended to contribute a set of improved instruments and techniques for use during the design of Solar PV off-grid hybrid systems and their operational management.

The study was limited to systems comprising renewable sources of PV, with diesel generator(s) as back-up and batteries as the storage technology. The study was limited to the many areas of Lesotho that would not, in the foreseeable future, be within reach of the national power grid and were made up of mini-grids as stipulated [6], [14].

1.6 Structure of the Thesis

The report of the research is made up of five chapters. This chapter (Introduction) gives the general background to the study; the problem statement, the objectives of the study, and the rationale for the study. Chapter 2 reports the results obtained from a literature review: it summarizes theories about rural access to electricity, discusses the development and design of mini-grids, solar photovoltaic designs, grid integration and demand forecasting, grid analysis and evaluation; all with due emphasis on the case points energy used in this study. Chapter 3 presents the methodology employed in this study, including the methods of data collection and validation, the design analysis procedures, the calculations, and the determinants of further optimization and subsequent evaluation. Chapter 4 presents the techno-analysis results and Chapter 5 presents conclusions reached from the interpretation of the results produced by the study.

Chapter 2: Literature Review

2.1 Introduction

This section contains a report of the results obtained from a critical review of the scientific literature relevant to this study. The topics explored included publications that pertained to Lesotho's electricity and energy situation, the promotion of the use of technologies utilizing renewable sources of energy, the application, and the design of off-the-grid solar systems, the merits of various options for their operations and design, load analysis and the economic analysis of energy systems, and solar system design optimization.

2.2 Energy Overview

According to various studies, Africa as a whole had one of the lowest levels of energy supply and consumption in the world. In 2013 for example, the Total Primary Energy Supply (TPES) for the world was approximately 13,500 Mtoe while the TPES for the whole of Africa only amounted to about 750 Mtoe (i.e. approximately 5.5% of the World TPES). This figure is even more striking when one considers the fact that the population of Africa at this stage was approximately 15% of the world's total population. The latest available data (2016) showed that the TPES for SADC Region was approximately 228 Mtoe [15]. The low energy consumption in Africa called for concerted efforts to boost the use of electricity (particularly when obtained from the use of clean modern energy) for economic growth and poverty reduction, without adversely affecting the environment.

In 2018 it was reported, by SE4All that in Lesotho energy was mainly sourced from Biomass, Coal, Petroleum, and Electricity. Biomass was Lesotho's main source of energy, as many households in Lesotho lacked access to electricity. Biomass (wood and dung) was used for cooking and space heating, especially in rural areas. Urban households were less reliant on biomass and mainly used paraffin and gas for space heating and cooking. Paraffin (kerosene) was mainly used for cooking, space heating, and lighting. Electricity was used primarily for lighting rather than for cooking and therefore represented a small proportion of domestic energy consumption. The use of solar energy such as solar power (Photovoltaic) (PV) for lighting was growing [3].

2.3 Electricity Access & Rural Electrification

A report published in 2018 pointed out that more than 60% of the population of SubSaharan Africa (SSA) was currently living in rural areas, and that projections indicated that the situation was not likely to change any time soon. Although SSA was rich in energy resources it had the lowest electrification rate in the world. The population of SSA was approximately 915 million people, of which only 290 million had access to modern energy services [2]. National electrification rates varied significantly among the Southern African Development Community (SADC) Member States (MS), where, in 2016, Mauritius and the Seychelles were either fully or almost fully electrified, but

Malawi had the lowest national electrification rate, at less than 10 percent. [15]

According to the Household Energy Consumption survey as quoted in the SEforALL Prospectus, Lesotho's Rural Electrification rate was only 11 % in 2017 [3]. As a result, many people living in rural areas in Lesotho face serious challenges, such as a lack of access to essential services like water, healthcare, education, and incomegenerating opportunities. On the other hand, fortunately, these people are located in places where solar power is the most abundant renewable energy resource available, and over 100 developing sites with high potential had been identified.

2.4 Solar Energy in Lesotho

Reports in 2001 and 2019 indicated that Lesotho was seen as a country with ample solar resource potential as shown in Figure 1: its Global Horizontal Irradiation (GHI) levels ranged from 1,826 kWh/m to 2,118 kWh/m per year depending on the location [16], [17]. The low latitude of the country resulted in a higher seasonality ranging from 10.5 daylight hours per day in winter to 13.5 daylight hours per day in summer. The solar resource was available over the whole year with more than 300 days of sunshine, except for rainy days when the performance of the PV systems may drop. Fernandez concluded in 2014 that the PV technology would be a "good fit" for Lesotho because of its cost-competitiveness, technological and market maturity, and for the fact that the country has a high annual availability of the solar resource. [6]

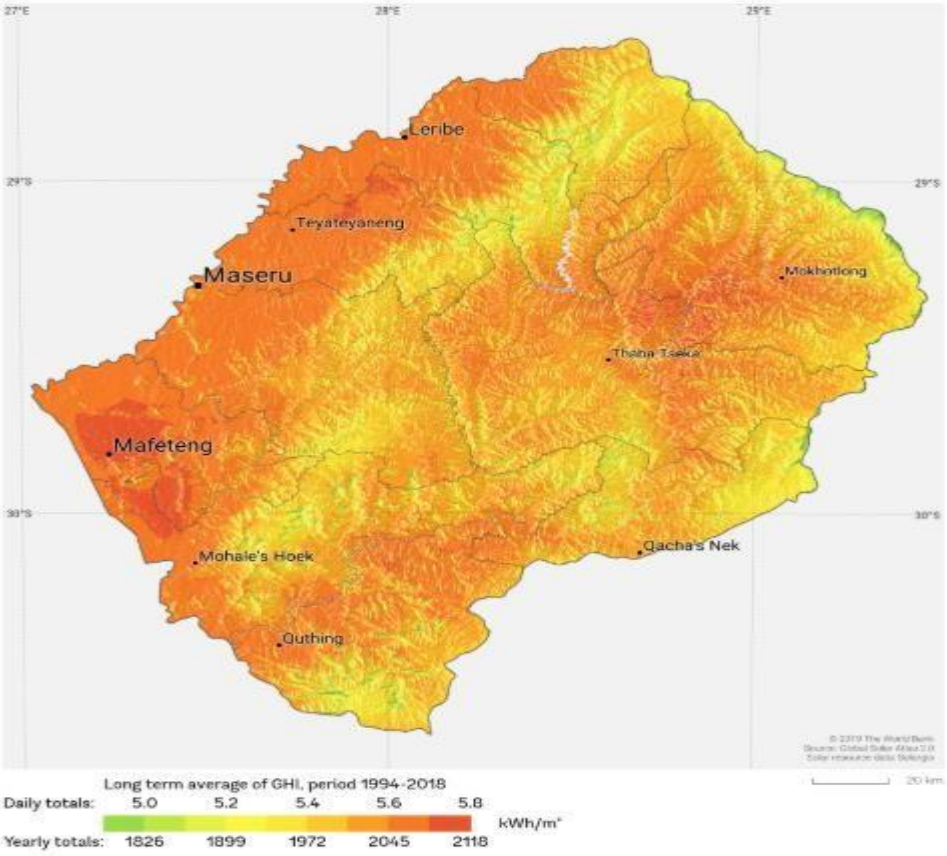

Figure 1 Radiation Map of Lesotho (Source: Global Solar Atlas)

2.5 Challenges of mini-grid implementations in developing countries

Multiple challenges continued to affect the successful deployment and operation of mini-grids in developing countries. Among the challenges reported in 2017 and 2018 were the high capital and operational costs coupled with a lack of access to affordable capital, the lack of regulatory clarity and laws, the tariffs that were either too high for local communities to afford or too low to generate revenues meeting the expectations of private investors, and the perceived lack of commercial sustainability [18], [19]. The challenges in Lesotho were the absence of an approved renewable energy policy [17] and the fact that the existing legal and regulatory framework relating to mini-grids was still not well-developed since no dedicated legislative existed that directly covered the mini-grids. Further challenges included the reality that the participation of the local private sector and the cooperative association in the energy business was limited, the coordination of endeavors in the energy sector was underdeveloped. In addition the institutional responsibilities for the energy efficiency programs and activities were

illdefined, thus leading to a loss of accountability [11], [20]. Also, there were no clear and transparent guidelines for the connection of mini-grids to the national grid and suitable compensation for it.

2.6 Opportunities for RE IPPs and Mini-grids

Over time, the Sub-Saharan countries such as South Africa carefully studied the extent and quality of their Renewable Energy (RE) resources. In the same vein, the Government of Lesotho itself and with the support of international agencies collected empirical and factual evidence of the nature, quantity, and quality of the available Renewable Energy (RE) resources of the country and made it available to policymakers, developers, investors, and financiers. Lesotho's abundant solar power resource indicated that there were unlimited opportunities available for RE-generated electricity. The report by Fernandez indicated that there were opportunities for minigrids, and there were 31 identified sites identified in Lesotho. Most of these places would be out-of-reach for the national power grid, because of the high-cost implications of electrification due to the unfavorable terrain, and therefore they could be seen as examples of the opportunities for mini-grids in Lesotho. [5]

Fernandez argued that the mountainous terrain and low population density, for example in the Senqu River Valley, the Foothills, and the Highlands of Lesotho rendered the extension of the national grid largely unfeasible, but justified electrification by off-grid means. The SEforALL report [21], stated that the gap between the peak demand and electricity supply in Lesotho had widened and had resulted in a supply deficit, mostly due to industrial development. As a consequence, therefore, amongst others, two electricity generation plants were proposed namely the 1200MW Kobong Pumped-Storage Scheme and the 1334MW Monontsa Pumped Storage Scheme. The use of Mini-grids as part of the pumped-storage plants may provide for additional transmission lines, which could later ensure another market for exporting electricity to Southern African countries.

2.7 Business models for rural mini-grids

Most of the business models for rural mini-grids used by, among others, the World Bank,and the UNDP were reported to be based on ownership of the mini-grid.

Community-based mini-grid management mainly occurred when a mini-grid, situated in an isolated area, did not attract the interest of the private-sector or a utility. In this case, the community became both the owner and the operator of the system and provided the maintenance, tariff collection, and management services. The establishment of private sector-led mini-grids was another possibility mentioned in the literature. These were often created when government support had raised an interest but they were sometimes also created spontaneously. Hybrid mini-grid models tried to combine different approaches to benefit from the advantages of each of the models and to minimize shortcomings. According to the World Bank, utilities were found to be the most common drivers for rural electrification in the developing countries [22], [23]

2.8 Benefits of a hybrid mini-grid

Drücke [22], argued that using a mix of different technologies from different energy sources would provide more competitive advantages than using a single technology. Some of these advantages became clear when some of the scenarios that a mini-grid had to cope with were examined. For instance, a mix of energy sources could accommodate seasonal fluctuations in the availability or quality of specific resources. Solar PV collectors could complement wind power during the months with less wind, or complement hydropower generation during the dry season. Where daily energy variations were concerned, solar energy production peaked around noon, while wind power facilities operated whenever the wind blew.

2.9 Design of hybrid mini-grid

Wiemann reported in 2011 that members of the Alliance for Rural Electrification (ARE) had been involved in the implementation of hundreds of mini-grid projects around the world [23]. ARE summarized the lessons learned from the projects in a report, which provided insights on the key issues to be considered when devising sustainable, replicable models for the scale-up of hybrid mini-grids. According to ARE a hybrid mini-grid system consisted of the production subsystem, the distribution subsystem, and the demand subsystem. ARE mentioned that each subsystem could have its architecture and specific set of components depending on the availability of resources, desired services required, and the users' characteristics [23].

The Production Subsystem included **generation** (Renewable Energy Technologies and Generator set), **storage** (batteries), **converters** (converters, rectifiers, and inverters to convert Direct Current (DC) power to Alternating Current (AC)), and **management components** (energy management systems) [24]. Wiemann explained that the Production Subsystem determined the capacity of the hybrid system to provide electricity, and connected all the components through the busbar (i.e. the electrical wiring connecting the different components) at the required voltage (AC/DC) for the Distribution Subsystem, which was in charge of distributing the produced electricity to the users utilizing the mini-grid [25]. It would be crucial to decide whether to use a distribution mini-grid based on DC or AC, a single-phase or three-phase grid since this decision could impact the cost of the project and ultimately determine the devices (appliances) which would be supported. The User (or application) Subsystem or Demand Subsystem included all the equipment on the end-user side of the system, such as meters, internal wiring, grounding, and the devices (appliances) which used the electricity generated by the hybrid power plant [23].

Wiemann pointed out that the design of the mini-grid directly affected the cost structure of the project and determined not only the price of the energy produced but also the quality of the services provided to the users. The early assessment phase of any successful design must integrate an analysis of the local conditions and the rural community's needs, and maximize the community's involvement and support of the design considerations. Local involvement was a necessity to reduce the chances of project failure and to prevent the forming of any negative images of the renewables in the region [23].

2.10 Costing Formulations

The World Bank (2007) published the results of an assessment of the then-current and then-future state of economic readiness of the electric power generation alternatives in the developing countries. The World Bank's report classified the power generation technologies into three distinct electricity delivery configurations (off-grid, mini-grid,

and grid) and then examined them critically. The generation technologies examined included Renewable Energy Technologies (RETs), and among these, also Photovoltaic (PV) Technology [25]. The report defined *generating cost* as the sum of *capital cost* and *operating cost*, expressed as a levelized unit cost (US$ per [kilo watt (s) per hour] kWh), where the levelizing was conducted over the economic life of the plant. Transmission costs and distribution costs were then expressed simply as the sum of their respective levelized capital cost plus O&M costs plus the cost of losses.

The Capacity Factor was defined as the ratio of the actual energy generated in a given period relative to the maximum possible if the generator produced its rated output all the time [25]. The Capacity Factor was a key performance characteristic, as it expressed the productive output relative to the installed capacity and allowed for capital costs to be expressed in levelized terms.

2.11 Hybrid Technologies and System Design Issues

2.10.1 Solar Photovoltaic (SPV) Systems

As quoted above, both Wiemann and the World Bank explained that Solar Photovoltaic (PV) generators converted the energy of the sun into electricity through their solar cells, which are semiconductor-based materials. A solar panel was formed by connecting solar cells. Each panel could have a peak capacity ranging from 80 W to 400 W, depending on its size and its technology. To achieve the desired output capacity, panels can be linked together [23], [25].

The energy produced by a PV generator was determined by the insolation at its location, in other words it was the amount of solar energy received at its specific location. Solar power resources were universally available at any location and the highest values could be achievable closer to the Equator. Therefore, PV systems in most developing countries tended to have higher performance than those in North America or Europe because of their closer proximity to the Equator. According to Wiemann [23], in North America, the insolation ranged from 1400 kWh/m^2 to 2300 kWh/m^2, whereas in Tanzania the values were around 2,500 kWh/m^2 and, in Afghanistan, approximately 2,000 kWh/m^2. The performance of PV was

sitedependent, but it was estimated that 1 kWp installed would produce more than 4 kWh per day.

Seasons were found to influence PV generation, and the time of day also influenced the production profile, as the peak production was found to happen at noon when the sun was perpendicular to the Earth's surface, but no production occurred during the night. The excess power produced during the day was stored in a battery for use when the sun was not available. As the PV generators produced DC power, extra components were necessary to adapt the voltage to that required by the applications. When batteries were included in a PV system, the PV generator would normally be connected to the batteries through a charge controller or a charger inverter. If, on the other hand, the PV generator was connected to an AC busbar feeder, it would require an inverter to adapt the voltage.

The Energy Sector Management Assistance Program (ESMAP) [25] reported in 2007 that the price of SPV technology had steadily decreased and that SPV technologies had gained many niche applications as result in such fields as satisfying the remote power needs for telecommunications, pumping, and lighting. SPV systems had many attractive features, including modularity, no fuel requirements, zero emissions, no noise, and no need for a grid connection.

2.10.2 Diesel generator set (Genset)

According to Wiemann (2011), diesel generators had been used widely in rural electrification for years, even though this technology was rarely, in the long run, the lowest-priced option (from a capital expenditure point of view). Diesel engines might run on natural gas (LPG), oil, or biofuels. Within hybrid power systems, the advantage of the diesel Genset was their dispatchability. Gensets improved the quality of service and the security of electricity supply as they were able to balance the intermittent production of the RETs. The Gensets would, for example, be working when renewables are not generating, or when the battery reached a low Stage of Charge (SoC). The "normal" life of a diesel generator was found to be from 3 to 5 years of continuous operation. In hybrid systems, the strategy was to use as little fuel as possible to reduce cost and to extend the life of the generator, ideally, to 20 years and more [23].

2.10.3 Storage (Batteries)

A battery, formed by a series of electrochemical cells, could be a significant cost factor of a hybrid power system. The battery was usually replaced every 6 to 8 years, but its life could be seriously reduced by improper operation and maintenance, and thus increased costs may result from its replacement. To improve the batteries' life the system had to be properly operated and maintained. A battery should, ideally, never be operated at levels below its stated minimum State of Charge (SoC). The mission of the battery was to provide power when the Renewable Energy Sources were unavailable. Knowledge of the frequency of the occurrence of the periods when renewable generation was interrupted, and an appreciation of the necessity to maintain the State Of Charge above the minimum, will be the basis for sizing the battery's capacity [23].

2.10.4 Mini-grid configuration

Components coupling (AC busbar)

Several authors indicated that the selection of the busbar depended on the technologies used in the system and on the energy management strategy. In hybrid mini-grids the use of AC busbars was more common when the battery was the central component of the system. A bidirectional master inverter could be installed to control the energy supply between AC loads and battery charge. In the case of an AC busbar the efficiency was higher, the losses lower and the system was more flexible and expandable, although the wiring was more complex [23] [26] [27], [28].

Single and three-phase distribution line

The distribution grid lines used either single-phase or three-phase. The use of threephase mainly allowed the connection of higher energy-consuming appliances which could, for example, be used for income-generating activities such as carpentry. The three-phase grid was more complex and needed more conductor lines, but was

also more easily expandable [22], [23]. The use of single-phase grids was found to have several advantages. For instance, the loads did not require to be balanced, and for the same size there was greater surge capacity. It also reduced the costs by allowing expansion of the generation capacity in the future. If only a few appliances in the village required three-phase electricity, it could be more cost-effective to invest in a phase converter instead of implementing a three-phase system [23].

2.11 Sizing the project

The extant literature seems to agree that the cost-efficient design of a hybrid power system had to match the production capacity and local demand exactly. Designing a system of over-sized capacity would result in unnecessary costs. The oversizing of the PV system generation capacity would increase the capital costs, which might be very high already, while producing a surplus of electricity which might not even be used. Furthermore the system might also be inefficient and reduce its life (e.g. an oversized battery might, most of the time, not charge fully and thus reduce the battery's life. An oversized PV module might overheat and thus reduce its efficiency and its life). In the case of diesel Gensets, oversizing could have a negative effect on the generator's life, as well as result in a higher fuel consumption rate, as Gensets were designed to run optimally at between 50-80% of their capacities [23]. Oversized battery banks were found to increase capital costs as well. On the other hand, under-sized generation capacity resulted in interruptions in the availability of power and caused dissatisfaction among end-users, which could lead to the failure of the RET project. Under-sizing could also increase the stress on the components, and reduce their lives. In short, the optimal sizing of the main components of an SPV system was found to be crucial to assure both the reliability of the electricity supply system and its cost affordability. Therefore, a poorly sized SPV system would negatively impact the Levelized Cost of Energy.

Two approaches to sizing stand-alone PV systems were reported, viz. the AverageDay Energy Balance approach, and the Time-Step Energy Balance approach. Of the two, the Average-Day Energy Balance approach was easier to use and required the input of less-sophisticated meteorological data, but was less exact and might lead to designing over-sized and costly PV systems. On the other hand, the Time-Step Energy

Balance approach required time-step (e.g. hourly data) meteorological and hourly load data, which were often not readily available. As a more exact approach, it allowed for estimating the reliability of the system's electricity supply and often resulted in designing systems which were more economical [29], [30].

2.12 Demand load dimension

Wiemann (2011) pointed out that to install a system with the correct production capacity, precise estimates of the output demanded from it, would be required. In a simplified way, the demand could be calculated by multiplying the number of users by the estimated average use of electricity per user. However, in this approach the margin of error was too large in the case of village-sized projects. Instead, it would be better to aggregate the estimated electricity demand of each potential user, by categories such as domestic, public services, and economic services [23].

Estimating electricity demand would require intensive door-to-door fieldwork. Two factors would be important, assessment of the user's willingness to be connected to the mini-grid and information about the estimated consumption by the electrical appliances that will be used once connected. Both of these factors would require a full understanding of the organizational, cultural, and ethnological structures of the rural community. It would be important to understand the role of men and women and their use of electricity depending on their daily tasks, the village's education needs, and so forth. Also, the demand could vary during the day and throughout the seasons of the year. Domestic users would use more electricity during evenings (for lighting, entertainment, education, and cooking), and reduce their use during the day. The distribution of the load over a week and the identification of the peak demand would be important as they would define the maximum capacity that the system has to produce at a specific instant. The hybrid mini-grid had to be prepared to meet the needs of all the users [23].

2.13 Load Management strategies

The main goal of a hybrid power system was to match the availability of resources with the demand for electricity. A combination of the selection of different technologies would be available, but it would be important to manage them effectively to maximize performance and, at the same time, to minimize costs. The literature study found several general guidelines related to the cost of electricity, which primarily focused on the use of fuel and the battery bank, and their effects on the life of the components and their replacement costs [23].

As a general rule, it emerged that the use of RETs for generating electricity was preferred to diesel generation. The marginal cost of generation with RETs was zero, whereas each kWh produced by the Genset required fuel and increased the cost of energy. Therefore the use of diesel Genset would be cost-effective mainly as a backup in cases where the production of the RETs was not sufficient to meet brief peak demand or when the battery had a low SoC [23].

To avoid damaging the battery, its SoC should not drop below its stated minimum SoC, as the battery could be seriously damaged, its life shortened and, as a result, premature replacement costs incurred. When very low levels of SoC were reached, Gensets could be used to address the situation. However, the life of the diesel generator would also be reduced by frequent on/off cycles since it had been recommended that for good performance the generator should be run at between 5080% of its capacity [23]. The management system should start the Genset when the battery approached the minimum SoC and let it run until the battery was fully charged again. Let us consider a typical scenario. In this situation the SoC levels dropped late at night, and the prescribed procedure was, that when the approaching low SoC was detected, the diesel generator would be started, and would be run until the battery was fully charged. The next morning, when the sun shone again, and because the battery was already fully charged, the PV generation was only used partially (e.g. catering for the actual consumption at the time). Clearly this approach would result in unnecessary fuel expenses. Another approach to this scenario could be not to have the generator running during the night until the battery was fully charged, and to accept that the battery would be subjected to increased stress for a short period until the users went to sleep. This approach would save on fuel costs and take advantage of the sun’s power to charge the battery in the morning [23].

2.14 Useful Standards for Hybrid Grids

Wiemann (2011) reported that the IEC Technical Specification Series 62257 was a comprehensive set of standards covering the technical and organizational aspects of mini-grids. These standards provided a comprehensive and logical framework for the design, installation, and maintenance of mini-grids, with a particular emphasis on safety, user-friendliness, and efficiency [23].

2.15 Solar Data products

In 2008, the existence of several subject databases containing data about radiation was reported, and they could be classified according to their data sources and how their data was processed. Some databases were collections of ground measurement data, others contained satellite data, and some databases organized the data (ground measurement and perhaps also satellite data) in spatial interpolation. Solar meteorological models that extracted satellite, atmospheric and meteorological data were usually less accurate, than good quality ground measurements. Their advantage was, however, their continuous geographical coverage and their ability to provide data about any location together with its a continuous history over periods of 10 to more than 20 years [31].

Cebecauer et al (2011) [32], provided a benchmark for solar radiation data products used in the then-contemporary software packages for the assessment of Photovoltaic (PV) systems. The software packages and the radiation products they used, were listed as follows:

1. Average daily profiles based on long-term monthly averaged values (e.g., ESRA, PVGIS, RETScreen);
2. Synthetic Time Series (e.g., Meteonorm, and PVSYST)
3. Typical Meteorological Year (e.g., PVWATTS, PVSYST, and SAM);
4. Aggregated Probability Statistics (SolarGIS, pvPlanner); and
5. Full Multiyear Series (e.g. SolarGIS (offline version)).

Monthly averages of daily profiles

For a quick estimate of the solar potential of a site, monthly averages of daily profiles would be used, represented by hourly, or even 15-minute, values [32]–[35].

Synthetic hourly time series

A method for generating synthetic hourly time series from long-term monthly averages reported by Aguiar and Collares-Pereira in 1992, was widely used, as was deemed a practical approach for generating an hourly time series from just 12 monthly values [36].

Typical Meteorological Year

In 2011 the Typical Meteorological Year (TMY) approach was used for real climate characterization, and several data sets were developed for some countries of Europe and America. For decades, TMYs had been used by engineers for simulation when building energy performance or solar systems. TMYs replaced the data covering many years with that of a single "typical" year, and this set was then used in applications such as PVWATTS and PVSYST [32].

Multiyear Time Series

A Multiyear Time Series could contain data purely measured on-site, or data derived purely from satellites or a combination of data obtained from both of these two sources. As a method of obtaining data about solar radiation, satellite-derivation was found to offer unsurpassed performance in terms of its availability, the quality of the data, its completeness, and the timeliness of delivery.

Aggregated Probabilistic Statistics

Cebecauer (2011) explained that, for PV simulations, the high-resolution solar and air temperature data pairs could be organized into percentiles and statistical bins according to the probability of their occurrence. Organizing the data in this way would use storage space more effectively for faster data accessing and quicker online processing for a selected site - enabling the optimal use of non-linearity in the simulations and increasing the speed and the accuracy of the computation.

After a thorough critical examination of the approaches and the data, Cebecauer concluded that, ideally, the Multiyear Time Series approach should be used for the proper modeling of the energy performance of a PV generator. It was further concluded that the closest choice to the Full-Time Series would be Aggregated Statistics, followed by Typical Meteorological Year (TMY).

2.16 Current theories

This section provides an overview of the theories found by the literature study.

2.16.1 Basics of Solar Geometry

The Earth-Sun distance increases and decreases during a year and the mean distance is approximately 1.496 x 10^{11} m. The maximum distance is about 1.521 x 10^{11} m and the minimum distance is about 1.471 x 10^{11} m [37].

2.16.2 Declination

The declination was the angular position of the sun at solar noon, with respect to the plane of the equator. Its value in degrees and is given by Equation 2.1 [38]–[41].

$$\delta = 23{,}45\sin\left[2\frac{284+n}{365}\right] \quad (2.1)$$

where *n* was the day of the year (i.e. *n* = 1 for January 1, *n* = 32 for February 1, etc.). Declination varied between -23.45° on December 21 and +23.45° on June 21 [42].

2.16.3 Solar hour angle and sunset hour angle

The solar hour angle was the angular displacement of the sun east or west of the local Meridian, which is negative in the morning, positive in the afternoon. The solar hour angle was equal to zero at solar noon and varied by 15 degrees per hour from solar noon. For example at 7 a.m. (solar time) the solar hour angle was equal to –75° (7 a.m. was five hours from noon; five times 15 equaled 75, with a negative sign because

it is morning) [38]–[43]. The sunset hour angle ω_S was the solar hour angle corresponding to the time when the sun sets [38]–[43]. It was given by the following Equation 2.2

$$\cos\omega_S = -\tan\phi\tan\delta \quad (2.2)$$

where δ was the declination, calculated through Equation 2.1, and ψ was the latitude of the site, specified by the user. The solar hour angle was given by Equation 2.3:

$$\omega = 15(t - 12) \quad (2.3)$$

2.16.4 Extraterrestrial radiation and clearness index

Solar radiation outside the earth's atmosphere was called extra-terrestrial radiation. Daily extra-terrestrial radiation on a horizontal surface (H_O), could be calculated for the n^{th} day of the year from the following Equation 2.4 [38]–[43]:

$$H_O = \frac{86400 G_{SC}}{\pi}\left(1 + 0.033\cos\left(\frac{2\pi n}{365}\right)\right)\left(\cos\phi\cos\delta\sin\omega_S + \frac{\pi\omega_S}{180}\sin\phi\sin\delta\right) \quad (2.4)$$

Where G_{sc} was the solar constant equal to 1,367 W/m^2. Before reaching the surface of the earth, radiation from the sun was attenuated by the atmosphere and the clouds [31], [38]–[43]. The ratio of solar radiation at the surface of the earth to extraterrestrial radiation was called the clearness index. Thus the monthly average clearness index, K_T, was defined by Equation 2.5:

$$K_T = \frac{\bar{H}}{H_O} \quad (2.5)$$

where H was the monthly average daily solar radiation on a horizontal surface and H_O was the monthly average extraterrestrial daily solar radiation on a horizontal surface [31], K_T values depended on the location and the time of year considered, and they were usually between 0.3 (for very overcast climates) and 0.8 (for very sunny locations).

The Efficiency of a PV panel was highly dependent on the amount of solar radiation received by the PV panel surface and the tilt of a solar panel influenced the gathered yield measurement. Therefore, solar panels would be inclined at ideal angles to gather the most extreme solar energy accessible in particular locations. Each location would have a specific tilt angle that differed from other locations, as the latitude of the location affected the tilt angle values.

2.17. Current models

2.17. 1 Solar PV Design and Simulation Software

According to IEA PVPS Task 11 [44], Off-grid PV systems and, in particular, hybrid PV systems were characterized (in 2011) by a high degree of complexity at the dimensioning stage. Therefore, as in many other fields, simulation software was an important aid. There was, then already, a broad diversity of such programs on the market. To get a worldwide overview of the available software tools and their features, a survey was initiated among the Task 11 participants to learn about the tools they were using. IEA PVPS Task 11 recommended that the key decisions to be made by the user when selecting a software tool concerned the desired focus of the calculations:

1. A preliminary feasibility study and general dimensioning (RETScreen),
2. Economic considerations (HOMER),
3. A detailed technical configuration (PV-SPS, PV*SOL, PVsyst)
4. System analysis (Hybrid2, PVDesignPro)
5. Detailed research (TRNSYS, MATLAB/Simulink).

2.17.2 Hourly Global Solar Radiation on Horizontal Surfaces

The global solar radiation on horizontal surfaces could be categorized as diffuse solar radiation (I_d) and direct beam solar radiation (I_b). Solar radiation on a horizontal surface was the sum of the horizontal direct and diffuse radiation as shown by Equation 2.6:

$$I_H = I_b + I_d \quad (2.6)$$

The diffuse solar radiation was the part of the sunlight that passed through the atmosphere and was consumed, scattered, or reflected by water vapor, dust particles, or pollution [45].

Most meteorological/radiometric stations normally measured the received global irradiation on horizontal surfaces. Collecting measurements in that way was quite expensive mainly due to the high cost of the measuring equipment. Therefore, mathematical models were developed to estimate diffuse radiation on horizontal surfaces. The models that determined diffuse radiation on horizontal surfaces were classified into *parametric models* and *decomposition models*.

Parametric models required specific information of environmental conditions such as atmospheric turbidity, fractional sunshine, cloud cover, and perceptible water content [46]. Decomposition models typically only utilized data about global radiation to estimate the diffuse radiation from the global solar radiation data. Decomposition models were based on a correlation between the diffuse and total radiation on a horizontal surface as given in Equation 2.8. The clearness index (k_t) was a measure of the atmospheric effects in an isolated place [47], and was a random parameter, it changed according to time of the year, season, climatic conditions, and the geographical situation of a place [48]. One of the decomposition models was that of Orgill and Hollands and it was reported in 1977. The correlation provided by Orgill and Hollands used four years' data gathered in Toronto, Canada [49]. Sky cover was categorized into three classes in this correlation, as follows:

For

$0 \le k_t \le 0.35, I_d = [1 - 0.249] I_H$;

$0.35 \le k_t \le 0.75, I_d = [1.577 - 1.84] I_H$; and

$0.75 \le k_t \le 1, I_d = [0.177] I_H$

2.17.3 Solar Radiation Models (Inclined Surface)

Data about the Solar radiation on the plane of the solar collector was required to estimate the efficiency of the collector and the actual amount of solar energy gathered. The total solar irradiance on a tilted surface could be divided into two components: (1) the beam component from direct irradiation of the tilted surface and (2) the diffuse component. The sum of these components equals the total irradiance on the tilted surface and is described in Equation 2.7:

$$I_T = I_{T,b} + I_{T,d} \qquad 2.7$$

Studies of clear skies led to an identification of the diffuse component composed of an isotropic diffuse component $I_{T,d,iso}$ (uniform irradiance from the skydome), circumsolar diffuse component $I_{T,d,cs}$ (resulting from the forward scattering of solar radiation concentrated in an area close to the sun), horizon brightening component $I_{T,d,hb}$ (concentrated in a band near the horizon and most pronounced in clear skies), and a reflected component that quantified the radiation reflected from the ground to the tilted surface $I_{T,d,g.}$ A more complete version of Equation 2.7 containing all diffuse components is given in Equation 2.8:

$$I_T = I_{T,b} + I_{T,d,iso} + I_{T,d,hb} + I_{T,d,g} + I_{T,d,cs} \qquad 2.8$$

The models all handled beam radiation in the same way, so that the major modeling differences were calculations of the diffuse radiation. Generally, diffuse radiation models for inclined surfaces could be classified into isotropic and anisotropic models. They differed in the division of the sky into regions with normal and elevated diffuse radiation intensities. Isotropic models assumed there was uniformity in the distribution

of diffuse radiation intensity over the sky. Anisotropic models included appropriate modules for representing areas of elevated diffuse radiation.

The isotropic sky model (Hottel and Woertz, (1942) (as cited by Duffie and Beckman, 1991; Liu and Jordan, 1960) was the simplest model and it assumed that all diffuse radiation was uniformly distributed over the skydome and that reflection from the ground was diffuse.

For an Anisotropic Model, such as the HDKR Model (2006), if the beam was reflected and all the terms of diffuse radiation such as isotropic, circumsolar and horizon brightening were added to the solar radiation equation, a new correlation developed called the HDKR model [16, 29] which was, basically, a combination of the models of Hay and Davies, and of Klucher and Reindl. The solar energy irradiation on the tilted surface was then determined by Equation 2.9:

$$\bar{H}_T = \bar{H}_b \bar{R}_b + \bar{H}_d A \bar{R}_b + \bar{H}_{\rho g}(1 - \cos 2\beta) \qquad \beta(H_d(1 - A(1 + \cos 2\beta)\sin^3(2\beta)$$

2.9

where

$\bar{H}_T$ is the monthly total incident radiation on a tilted surface;

$\bar{H}_b$ is monthly mean daily beam radiation on a horizontal surface;

$\bar{H}_d$ is monthly mean daily diffuse radiation;

$\bar{R}_b$ is the ratio of mean daily beam radiation on the tilted surface to that on a horizontal surface;

$\bar{H}_{\rho g}$ is diffuse reflectance from the ground;

β is representing the slope of the PV array;

A is an anisotropy index which is the function of transmittance of the atmosphere for beam radiation and defined as:

$$A = \frac{\overline{H^b}}{H_o} \qquad 2.10$$

According to [37] (2011) the Actual Albedo (ground reflectance)values ρ were derived from satellite images by evaluating brightness values. The data series of the measured albedo values for a given place were used to determine the local ground albedoρ_{min}, which was defined as the minimal reflectance shown by the images. The ground albedo had to be identified for every site individually because it varied by surface conditions. The identification of reflectance values equal to the ground albedo was then assumed to correspond to clear sky conditions. The maximal albedoρ_{max}, which corresponded to a totally-overcast sky, did not have to be identified individually at every site, because it did not depend on ground conditions, but depended exclusively on the incident angle. The actual reflectance (ρ) at a given place and time must be between the local minimal reflectance (ground albedo) ρ_{min} and the general maximal reflectanceρ_{max}. The cloud index n indicated the value of ρ in relation to ρ_{min} andρ_{max}. It was defined as shown by Equation 2.11 [37], [50]:

$$n = \frac{\rho - \rho^{min}}{\rho_{max} - \rho_{min}} \qquad 2.11$$

Gunther (2011) [37], further pointed out that the ground albedo of a given place may change over time due to changing vegetation conditions. Taylor and Stowe (1984) [51] derived Equation 2.12:

$$\rho_{max} = 0.78 + 0.13(1 - e^{-4\cos\theta_Z - 5}) \qquad 2.12$$

Gunther suggested that, for different ranges of n, k_t is determined in the following way:

For

$$n \square\square 0.2, K_t \square 1.2;$$

$$\square 0.2 \square n \square 0.8, k_t \square 1 \square n;$$

$$0.8 \square n \square 1.1, k_t \square 0.05 \text{ ; and}$$

$$1.1 \square n, k_t \square 0.05$$

where n was the cloudiness index and k_t was the clearness index, the ratio of actual global irradiance to clear sky global irradiance.

2.17.4 Other models

Cicilio et al [52], performed a case study using a toolset call uGrid to design a minigrid for the Ha Makebe village in Lesotho, which highlighted pole placement capabilities and changes in network layouts over a range of reliability probabilities. uGrid was a tool created by the minigrid developer OnePower in Lesotho to perform resource allocation and sizing optimization of energy generation infrastructure based on statistical load estimates. Cicilio concluded that the toolset closed a gap for flexible and affordable holistic minigrid planning, needed by minigrid developers.

2.18 Photovoltaic Generator Power Output Model

Some recent (2016 to 2019) sources indicated that the PV systems produce power in proportion to the sunlight striking the solar array surface. The actual output of a solar power system could vary substantially as the intensity of the light on a surface varied throughout a day, as well as from one day to another. The Solar PV Power (*PPV*) output was given by Equation 2.13 [29], [53]–[55]:

$$P_{PV} = \frac{\eta_{PV}}{} \cdot \frac{G_T}{} \cdot \eta_{STC} G_{STC} \qquad P_{array} \qquad (2.13)$$

where

η_{PV} is the instantaneous cell-temperature-dependent PV efficiency

η_{STC} is the PV efficiency at standard test conditions (STC)

G_T is the solar irradiance incident on the plane of the PV array/module

G_{STC} is the in-plane incident solar irradiance at standard test conditions P_{array} is the power output from the PV array.

2.18.1 PV field efficiency (η_{PV})

Hove [29], developed a model which could be used to determine the Instantaneous PV Efficiency directly from the meteorological conditions (solar irradiance and ambient temperature) and the measured characteristics of the PV module ($\eta_{mp,STC}$, $T_{c,NOCT}$, β, etc.). Using this model one would not need to calculate the cell temperature first before determining the Instantaneous PV Efficiency. The Instantaneous PV Efficiency model could be expressed by Equation 2.14 as:

$$\eta mp = \eta mp,STC\,[1 - 0.9\beta\, G\frac{G^T}{}_{T,NOCT}\,(T_{C,NOCT} - T_{a,NOCT}) - \beta(T_a - T_{C,STC})]$$

2.14

where η_{mp} is the instantaneous PV efficiency

$\eta_{mp,STC}$ is the maximum power point efficiency under standard test conditions

β is the temperature coefficient of power [%/°C]

G_T is the solar irradiance incident on the plane of the PV array/module

$G_{T,\,NOCT}$ is the solar radiation at which the NOCT is defined [0.8 kW/m2] $T_{c,\,NOCT}$ is the nominal operating cell temperature [°C]

$T_{a,\,NOCT}$ is the ambient temperature at which the NOCT is defined [20°C]

T_a is the ambient temperature

$T_{c,\,STC}$ is the cell temperature under standard test conditions [25°C]

2.18.2 The Ratio of Beam Radiation on a Tilted Surface to that on a Horizontal Surface, R_b

Calculating the hourly radiation on a tilted surface of a collector to that on a horizontal surface was often necessary for purposes of designing the solar process and for calculating its performance. The most commonly available solar radiation data was expressed in hours or days on a horizontal surface, whereas the need was for beam and diffuse radiation on the (tilted) plane of the collector. The ratio R_b was locationdependent, day-of-year dependent, and time-of-day dependent and could be calculated analytically from solar geometry as shown in Equation 2.15:

$$R_b = \frac{cos\theta}{cos\theta_z}$$

$$cos\theta = sin\delta sin\varphi cos\beta - sin\delta cos\varphi sin\beta cos\gamma + cos\delta cos\varphi cos\beta cos\omega + cos\delta sin\varphi sin\beta cos\gamma cos\omega + cos\delta sin\beta sin\gamma sin\omega$$

$$cos\theta_z = sin\delta sin\varphi + cos\delta cos\varphi cos\omega \qquad 2.15$$

where

R_b is a geometric factor defined as the ratio of beam radiation on the tilted surface to that on the horizontal surface;

θ is the angle of incidence of beam radiation on the tilted surface; and

θ_z is the zenith angle or angle of incidence of beam radiation on the horizontal surface;

 is the surface azimuth angle**,** the angle between the plane of the surface in question and the horizontal;

ω is the angle, the angular displacement of the sun east or west of the local meridian due to the rotation of the earth on its axis at 15^o per hour.

 Is the latitude, the angular position north or south of the equator, north positive;

δ is the declination, the angular position of the sun at solar noon with respect to the respect to the equatorial plane

β is the angle between the plane of the surface in question and the horizontal.

2.18.3 Energy yield

According to Thevenard and Driesse [56], energy production, or yield, was of primary importance to large-scale PV projects because it directly determined the revenue. The sun, justifiably regarded as a quite-stable source of input energy, was nevertheless subject to local, seasonal and year-to-year variations. Thevenard pointed out that it was therefore easy for developers to be over-confident about the yield predicted by the simulation programs, without realizing the uncertainties attached to these predictions. The use of even the methods available would entail a level of uncertainty that was significant to the developers. They suggested [56], that the uncertainties related mainly to the evaluation of the solar resource and to the performance of the system itself, were typically 4% for year-to-year climate variability, 5% for solar resource estimation (in a horizontal plane), 3% for estimation of radiation on the plane of the array, 3% for the power rating of the modules, 2% for losses due to dirt and soiling, 1.5% for losses due to snow, and 5% for other sources of error. A Monte-Carlo type of simulation was used to determine the combined effect of these uncertainties on the annual yield of a typical large PV farm in Ontario. It was found that the combined uncertainty (in an RMSE sense) was of the order of 8.7% for individual years, and 7.9% for the average yield over a 20-year system-lifetime.

2.19 Levelised Cost Of Electricity (LCOE) Calculations

According to Pueyo (2016), the LCOE measured the total cost of producing a kilowatthour (kWh) of electricity over the lifetime of a project using Equation 2.16 [57]. The total cost over the project life would be divided by the amount of electricity generated over the same period, to give an average cost, usually expressed in US cents per kWh. Costs comprised capital investment, operating and maintenance (O&M) costs, and decommissioning costs. All these costs and the total generation per year would be discounted to a reference date using a discounting rate that reflects the cost of capital.

$$LCOE = \frac{I_o + \sum_{nt=1} \frac{(1A+ti)t}{}}{\sum_{t=0}^{n} \frac{Mt,el}{(1+i)t}} \quad 2.16$$

where

I_0 is the Investment (or capital) costs in common currency;

At is the Annual total costs in year t in common currency;

, is the Produced quantity of electricity in the respective year in kWh;

i is the Discount rate;

n is the Operational lifetime in years;

t is the Year of the lifetime (1, 2, ...).

The De-risking Renewable Energy Investment (DREI) report's approach for LCOE calculations would take an equity investor's viewpoint to the LCOE and would also use NREL [47],[48]. The equation shown in Figure 2, sets out the LCOE formula to be used: a capital structure (debt and equity) would be determined for the investment and the cost of equity would be used to discount the after-tax cash flows to the equity investors.

$$\frac{\%\ \text{Equity Capital} * \text{Total Investment} + \sum_{T=1}^{T} \frac{(O\&M\ Expense)_t + (Debt\ Financing\ Costs)_t - Tax\ Rate * (Interest\ Expense_t + Depreciation_t + O\&M\ Expense_t)}{(1 + Cost\ of\ \text{Equity})^t}}{\sum_{T=1}^{T} \frac{Electricity\ Production_t * (1 - Tax\ Rate)}{(1 + Cost\ of\ \text{Equity})^t}}$$

Where,
% Equity Capital = portion of the investment funded by equity investors
O&M Expense = operations and maintenance expenses
Debt Financing Costs = interest & principal payments on debt
Depreciation = depreciation on fixed assets
Cost of Equity = after-tax target equity IRR

Figure 2 DREI report's approach for LCOE calculations

2.20 Economic analysis

In determining the optimal solution based on Lowest Cost of Energy and Net Present Cost, the Cost of Energy would be calculated using Equation 2.17, where CA_cap is the annualized capital cost, CA_rep is the annualized replacement cost, $CA\_O\&M$ is the annualized Operation and Maintenance cost ($CA\_O\&M$) of the system components, and Es is the energy served in a year [43]:

$$COE = C\frac{C_{A\_cap}+C_{A\_rep}+C_{A\_O\&M}}{Es} \quad 2.17$$

On the other hand, the Net Present Cost would be determined from Equation 2.18, where *CRF (i,n)* is the capital recovery factor determined from Equation 2.19, where *i* is the real annual interest rate and *n* is the number of years [60]:

$$NPC = C\frac{C_{A\_cap}+C_{A\_rep}+C_{A\_O\&M}}{CRF(i.n)} \quad 2.18$$

$$CRF(i,n) = (\frac{i(1+i)^n}{1+i)_{n-1}} \quad 2.19$$

The annual real interest rate *i* would be calculated by Equation 2.20:

$$i = \frac{i-f}{1+f} \quad 2.20$$

where the nominal interest rate was i and *f* was the annual inflation rate.

Chapter3: Methodology

This section provides the details of the methodological approach used in this study, to obtain, compute, simulate, and analyze appropriate information to achieve the objectives stated in section 1.4 It presents specifics of the components-modeling approach, solar resource accessing and predicting of the energy yield of the PV system, the construction of the load profiles, the energy management processing, and optimization methods, calculating the actual system components, and the approach to designing an optimum system.

This study set out to design a PV-Diesel based hybrid power generation system with battery storage. Figure 3 below presents a schematic diagram of the conceptual design of the proposed off-grid hybrid system. The PV array is connected to a solar inverter that is connected to the AC bus together with the diesel generator along with the load demand. The AC bus also connects the battery bank which exchanges power via a bi-directional inverter charger. After meeting the load demand, the surplus energy from the PV system and the diesel generator is used to charge the battery bank up to the point when the battery bank's State of Charge reaches its maximum value of 1. The additional energy generated exceeding the maximum State of Charge of the battery bank is dumped. In other situations, the additional energy (dumped) could be supplied to the grid, but this feature was beyond the scope of this study as this was intended to be an off-grid system. Here a simple spreadsheet-based simulation model was designed to determine the feasibility of a system with lower Cost of Energy (COE) and reliability of supply over the 8760 hours in a year.

The Excel spreadsheet model was used in three different stages. In the first stage, the load requirements and meteorological data were appropriately estimated. The technical and economic characteristics of different hardware components were selected as input parameters into the model. The operating strategy used was the cycle charging (CC) strategy. In the second stage, the model performed a simulation based on the energy balance to meet the specific set of technical and economic constraints. It should be noted that the model provided important performance indicators to evaluate and compare the designed systems.

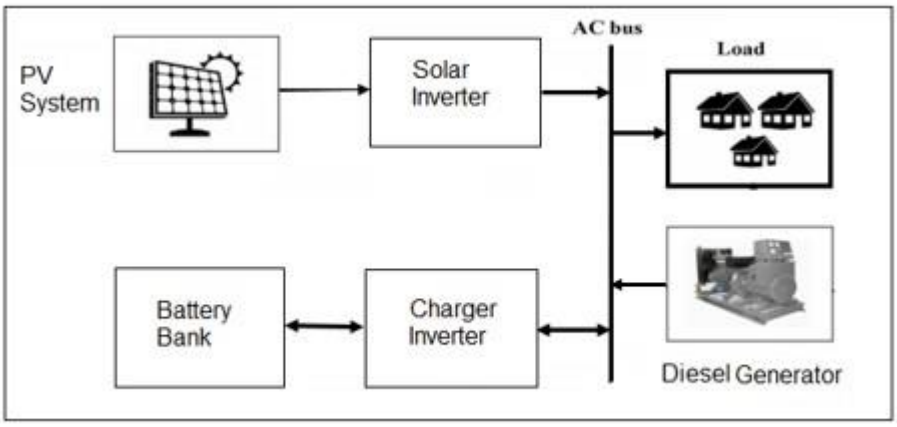

Figure 3 Schematic diagram of the PV/Diesel system with Li-ion Battery storage

3.1 Meteorological data

The study considered the case of a typical village location, remotely located, and the village selected was Riabaneng in the district of Mohale's Hoek Lesotho (Latitude: 29.844, Longitude: 27.663). The proposed area was not connected to the national grid and kerosene, candles, and biomass were the resources used for lighting and cooking. The required hourly meteorological data were obtained from (https://re.jrc.ec.europa.eu/pvg_tools/en/tools.html#TMY), the Typical Meteorological Year database. The model determined the P_{PV} (power output of the solar PV array at any given time) by calculating the incident irradiance (G_T) which required the global horizontal irradiance (GHI), the diffuse horizontal irradiance (DHI), and other meteorological variables such as ambient temperature and day number.

3.2 System Components modeling

3.2.1 PV array modeling

Photovoltaic Generator Power Output Modeling

The essential inputs required to calculate the PV array output included the day of the year, location-specific information (e.g. latitude, and longitude), weather information (e.g. solar irradiance), ambient temperature, clearness index and PV-systems-related information (e.g. the orientation of the array and the array size). Some performancerelated characteristics were also required, such as the PV inverter's manufacturer,s specifications. The total (global) irradiance incident on the horizontal surface of a PV array (the plane of the array) is the arithmetic sum of the direct (beam) and diffuse irradiance components incident on a horizontal surface, as shown in Equation 2.6.

Determination of Incident Solar Radiation on a Tilted Surface

The incident solar irradiation on the tilted surface was the sum of a set of radiation streams including beam radiation, the three components of diffuse radiation from the sky, and the radiation reflected from the various surfaces seen by the tilted surface. The total incident radiation on the tilted surface was obtained from the use of Equation 2.7.

The declination (□) was calculated using Equation 2.1, where the day number (*n)* was obtained from Table 14*.* The solar hour angle (ω) was also calculated using Equation 2.3, with the hour (t) computed from Table 14. Therefore, R_b was calculated using Equations 2.15. Using Equation 2.6 the hourly I_b values were calculated using the global horizontal irradiance (GHI) and the diffuse horizontal irradiance (DHI) in Table 14. The hourly diffuse reflectance from the ground ($I_{\rho g}$) was calculated using

Equations 2.11 and 2.12. The solar energy hourly irradiation on the tilted surface was then determined by substitution in Equation 2.9. Tables 4.1-4.3 show all the results that were thus obtained in this process.

$$I_T = I_b + I_d A R_b + I_{\rho g}\left(1 - \cos 2\beta\right) + I_d\left(1 + A\right)\left(1 - \cos\beta\right)\left(1 + \sin^3\left(\frac{2\beta}{2}\right)\right) \quad 3.1$$

Measured PV module characteristics

The variables needed to completely evaluate the PV Generator Model of Equation 2.13 were obtained from measurements recorded on the PV module datasheet. These variables were the module rated power, $\boldsymbol{P_{STC}}$ **;** the module maximum efficiency at STC, $\boldsymbol{\eta_{STC}}$ **,** which might also be obtained by dividing the rated power by the module area and the STC irradiance $\boldsymbol{G_{STC}} =$ 1000 W/m^2; the nominal operating cell temperature, $\boldsymbol{T_{C,NOCT}}$**;** the ambient temperature for the NOCT test, $\boldsymbol{T_{a,NOCT}} = \mathbf{20}$℃ and the cell temperature at STC test conditions, $\boldsymbol{T_{C,STC}} = \mathbf{25}$℃**.**

To simulate the hourly performance of the module over the day with meteorological variables of Table 14, the relevant test variables were assumed to be. $P_{STC} = 345\ W$; $\eta_{STC} = 18\%$; $G_{STC} = 1000\ W/m2$; $T_{C,NOCT} = 43$℃; $T_{a,NOCT} = 20$℃; $T_{C,STC} = 25$℃; $\beta = 0.005$; $G_{T,NOCT} = 800\ W/m^2$.

PV field efficiency (η_{PV})

Therefore, given the ambient temperature $\boldsymbol{T_a}$, the incidence irradiance $\boldsymbol{G_T}$ and the measured PV module characteristics$\eta_{mp,STC}$, $T_{c,NOCT}$ and β, Equation 2.14 was used to evaluate the hourly variation of efficiency.

PV array Energy (E_{PV})

The power output from the PV array was calculated as a product of the dimensionless variable ($\frac{P}{P_O}$) representing the PV component size and the daily average load ($\frac{L_d}{24}$) as shown by Equation 3.2.

$$E_{PV} = \frac{P}{P_O} \times \frac{L_d}{24} \qquad 3.2$$

To allow for the uncertainties associated with the prediction of long-term photovoltaic (PV) yield as summarized by Thevenard and Driesse [56], a combined uncertainty of the order of 8.7% for individual years was applied to Equation 2.13.

3.2.2 Diesel generator (DG) modeling

The diesel generator capacity was determined by first assuming the peak demand of the generic village, with an additional safety margin of 20% added on. The minimum load factor for the diesel generator to protect it from damage when loads were below a certain threshold, was assumed to be 30%. If diesel engines were to run below the recommended minimum loading level for an extended period, it would result in low efficiency and cylinder bore glazing. This would reduce the engines' operating life, and increase their annual operational and maintenance costs. The fuel consumption of the DG (Fc) was modeled according to Equation3.3 as a function of the amount of electricity generated (kWh), given efficiency (ɳ), the calorific value of the diesel (kJ/kg) and the density of the diesel (kg/L).

$$\mathrm{Fc\ (l)} = \frac{E_{gen}\ (kWh)}{\eta\ (\%) \times CD_w\ (kWh/l)}$$

$$CD_w(kWh/l) = CD_J\ (kJ/kg) \times D_d(kg/l) \qquad 3.3$$

The values used for the efficiency (ɳ), the calorific value of diesel (kJ/kg), and the density of diesel (kg/L) were 30%, 44,800, and 0.832 respectively.

The constraint for the generator was given by:

$$P_{DGmin} \geq P_{DG}(t) \geq P_{DGrated} \qquad 3.4$$

where $P_{DG}(t)$ represents instantaneous power from the DG unit, P_{DGmin} and $P_{DGrated}$ represented the minimum allowable power output from the DG unit and the rated power of the DG unit, respectively,

3.2.3 Battery Bank (BB) modeling

A battery model based on Li-ion technology was used in this study. The inputs were the battery string size (Wh), the initial and minimum State of Charge (SOC) of the battery bank, and specified roundtrip efficiency. The battery State of Charge (SOC) at a specific time was given by Equation 3.5 as follows:

$$SOC(t) = SOC(0) + \eta_c \sum_{k=0}^{t} P_{CB}(t) + \eta_d \sum_{k=0}^{t} P_{DB}(t) \quad 3.5$$

Where, *SOC(0)* is the State of Charge of the battery at *t = 0*, P_{CB} is the electrical power charged in the battery, P_{DB} is the electrical power discharged from the battery bank, η_c and η_d are respectively the charging and discharge efficiencies. During charging/discharging, the SOC limit was always checked for the battery systems using Equation 3.6.

$$B_{min} \leq SOC(t) \leq B_{max}$$

$$B_{min} = (1 - DOD)B_{max} \quad 3.6$$

where, the minimum and the maximum power capacity of the battery were respectively B_{min} and B_{max}, and *DOD* is the Depth of Discharge. The discharge power of the battery bank had the following constraint [32-33]:

$$0 \leq P_{DB}(k) \leq P_{\max} \quad 3.7$$

where P_{max} is the maximum hourly discharging power

3.2.4 Inverter modeling

It was assumed in the modeling that all the inverters were integrated with the individual system components. The inverters dedicated to the battery banks were bi-directional inverter chargers, and the dedicated inverters that were coupled to the PV arrays were PV solar inverters. Equations 3.8 and 3.9 showed the basic mathematical expressions used for calculating the inverter's uni-directional input and output power.

$$P_{inv-BB}(i) = P_{BB}(i) \times \eta_{inv} \quad 3.8$$

$$P_{inv-PV}(i) = P_{PV}(i) \times \eta_{inv} \quad 3.9$$

where P_{PV} was the output power of the PV array (kW), P_{BB} was the output power of the BB (kW), − $P_{inv\text{-}BB}$ was the input/output power of the battery inverter, − $P_{inv\text{-}PV}$ was the input/output power from the solar inverter and η_{inv} was the inverter efficiency.

3.3 Load profile

The expected use of electricity was divided into three categories; Domestic Use, Productive Use, and Public Use. The socio-demographic issues of the users considered for this exercise, were: the ownership of the appliances and their usage, cooking habits, usage of alternative fuels, the demographics of the members of the household (e.g. age, education, and employment), household income, potential types of business, and availability of public institutions. The categories were further disaggregated to improve the validity of the estimates.

The appliances which could be employed in this village were sorted into six groups as shown in Table 1 and then arranged in a way to make it easier to find suitable common appliances for each customer type. The appliance types were Lighting, Domestic uses, Commercial gadgets, Office equipment, Health Care Equipment and Electric machines. The appliances each received further descriptors of their characteristics: its power demand, the type of usage (deterministic, stochastic, and critical-stochastic) and, finally, the time when it would be used. The deterministic loads applied to loads of which both the size and the time of its impact were known, stochastic loads referred to loads of which the size was known but the time of its impact was unknown, and critical indicated loads the demand of which must always be met. The different types of loads to be connected to the system were grouped as follows:

- Duty Cycle Appliances were appliances which turned themselves on and off automatically (e.g. refrigerators);

- Base Load Equipment were equipment or appliances which were normally powered on
  all the time (like communication equipment);
- Scheduled Equipment were equipment or appliances like lights and computers which normally functioned at predetermined times;
- Phantom Loads were loads caused by any appliance that consumed power even when it was turned off.

Table 1 Appliance sorting

Appliances & Equipment	Power Demand	Type of load	Usage	
			Type of usage	Time of usage
Lighting				
Indoor light	20 W	Scheduled	Deterministic	from 6pm till 11pm or until closing
Working light	20 W	Scheduled	Deterministic	time during working hours
Outdoor light	11 W	Scheduled	Deterministic	from 6pm till 11pm or until closing
Security light	11 W	Scheduled	Deterministic	timefrom 6pm or when closing till 6am
Domestic appliances				or when opening
Radio small	30 W	Phantom (5.44W)	Deterministic	during working hours
Radio big	150 W	Phantom (5.44W)	Deterministic	during working hours
Small Hot Plate-High/low	1500 W	Duty cycle	Stochastic	during working hours
Kettle	2000W	Scheduled	Stochastic	during working hours
TV	100W	Phantom (25W)	Stochastic	follows working hours
Flat screen TV	180W	Phantom (35 W)	Stochastic	follows working hours
DSTV Decoder	100 W	Phantom (25W)	Stochastic	follows working hours
DVD player	80W	Phantom (10.58)	Deterministic,	follows working hours
Iron	2000W	Scheduled	Stochastic	during working hours
Phone Charging	8W	Scheduled	Stochastic	during working hours
Commercial appliances				
Welding	9000W	Scheduled	Critic Stochastic	During working hours
Power drill	500W	Scheduled	Stochastic	During working hours
Angle grinder	900W	Scheduled	Stochastic	During working hours
Big grinder	2000W	Scheduled	Stochastic	During working hours
Refrigerator	200 W	Duty cycle	Stochastic	24 hrs
etc				
Office appliances				
Computer	200	Scheduled	Critic Stochastic	During working hours
Printer	100	Scheduled	Stochastic	During working hours
Photo copier	100	Scheduled	Stochastic	During working hours
Health Care appliances				
Examine. Lamp	40W	Scheduled	Critic Stochastic	During working hours
Microscope	20W	Scheduled	Stochastic	During working hours
Hot plate	2000W	Scheduled	Stochastic	During working hours
Boiler Large	1000W	Scheduled	Stochastic	During working hours
Bar Fridge	100W	Duty cycle	Stochastic	24 hours
Communication equipment	100W	Base load	Stochastic	During working hours

Electric Machines				
Milling Without load	7000W	Starting surge	Critic Stochastic	During working hours
Milling with load	12500W	Starting surge	Critic Stochastic	During working hours

A novel concept called the “Demand Matrix Method”, was used to construct load profiles based on the appliance list and ratings. The Appliance Power Matrix was developed which involved appliance time-of-use scheduling. Table 2 shows the number of customers, the appliance/equipment list, the appliances, and the quantity. The power rating (in watts) is also indicated and the total power was obtained from multiplying the number of appliances, the number of customers, and the nominal power rating. This was then taken to be a N_a*1 matrix called $\boldsymbol{M_1}$.

Table 2 Appliance Power (M_1) Matrix Sample

Public Uses		Quantity of appliances		Power_ of_ Appliance			
Type of Use	No. of users	Quantity Appliance	Results _1	Duration of Use	Power Rating (W)	Power	Results_ 2
Schools	a						
Deterministic							
Indoor light	a	x	ax	b	y	by	axby
Working light	a	x	ax	b	y	by	axby
Radio small	a	x	ax	b	y	by	axby
Stochastic							
Phone Charging	a	x	ax	b	y	by	axby
Computer	a	x	ax	b	y	by	axby
Printer	a	x	ax	b	y	by	axby
Photo copier	a	x	ax	b	y	by	axby
Laptop	a	x	ax	b	y	by	axby

Subsequently, the Time-of-Use Matrix which indicated the time of day and the appliances in use for the hour was established (Table 3). A prediction of the usage hours and their distribution over a 24-hour cycle is shown in the demand matrix ($\boldsymbol{M_2}$) in Table 3. The time-of-day and the appliance-in-use at the same hour, are indicated, where each role is assigned to a unit hour; hence 24 roles represent a 24-hour (full day) cycle. The number of appliances of the same type being operated at the same time was given as a percentage i.e. the number of lights expected to be operational during the night is 100%, given as “1” in the Time of Use matrix.

Table 3 Time of Use Matrix (M_2)

Appliances	**Hours of day**														
	1	**2**	**3**	**4**	**5**	**6**	**7**	**8**	******	**19**	**20**	**21**	**22**	**23**	**24**
Schools									**						
Deterministic									**						
Indoor light									**	1	1	1			
Working light							1	1	**						
Outdoor light	1	1	1	1	1	1			**	1	1	1	1	1	1
Stochastic									**						
Phone Charging							1	1	**						
Computer							1	1	**						
Printer							1	1	**						
Photo copier							1	1	**						
Laptop							1	1	**						

The ***M_2*** matrix, was then multiplied by the ***M_1*** matrix to give a 24*1 matrix that represents the hour load profile, M3, (Table 4). The resulting load profile, representing the deterministic load, the stochastic load, and the critic load was obtained from plotting instantaneous hourly power demand against time as shown in Figure 4.

Table 4 Hourly Load Profile Matrix

Appliances	**Hours of day**															**Total Daily power consumtion (W)**
	1	2	3	4	5	6	7	8	9	10	xx	21	22	23	24	

Schools											xx					
Deterministic	10	10	10	10	10	10	10	10	10	10	xx	20	10	10	10	
Indoor light											xx	10				40
Working light							10	10	10	10	xx					110
Outdoor light	10	10	10	10	10	10					xx	10	10	10	10	130
Stochastic	0	0	0	0	0	0	50	50	50	50	xx	0	0	0	0	
Phone Charging							10	10	10	10	xx					110
Computer							10	10	10	10	xx					110
Printer							10	10	10	10	xx					110
Photo copier							10	10	10	10	xx					110
Laptop							10	10	10	10	xx					110
Critical	0	0	0	0	0	0	0	0	80	80	xx	0	0	0	0	830
Total Power (W)	10	10	10	10	10	10	60	60	140	140	xx	20	10	10	10	1660

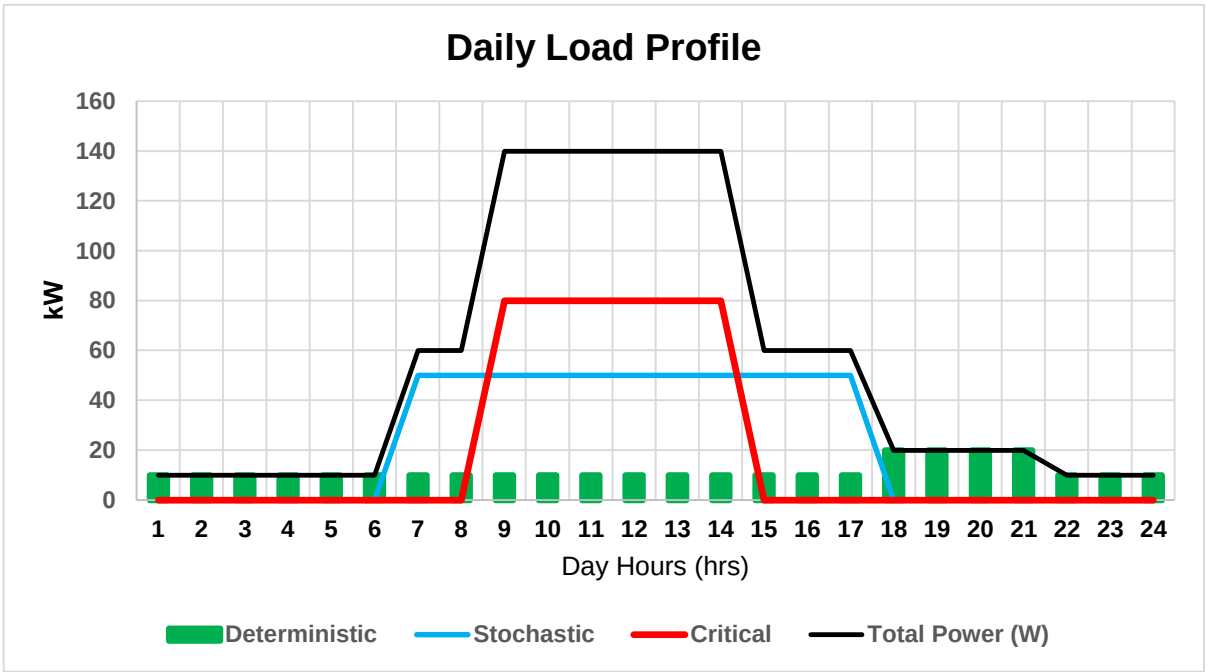

Figure 4 Daily Load Profile

3.4 Energy management

A high-level flowchart of the operation of the energy management process is shown in Figure 5. At each hour, the capacity of the hybrid system is the sum of all the power generated by the system relative to the amount of stored energy. To meet the electricity demand, the output power produced by the PV system would be used and in the event of a power deficit, the storage system would run to satisfy the shortfall. If the load demand is then still not completely met, the DG system would be turned on. If after this step, the load was still not entirely met, there would be an “unmet load situation”. Depending on the amount of the power produced and the load demand, one of the following states (A or B) might occur. The steps of the energy management process could be explained in detail as follows:

A. If $\boldsymbol{\eta_{inv1} \times P_{pv}\ (t) \geq P_L\ (t)}$, then the electrical load was entirely supplied and there would be excess power. The excess power produced by the PV system (P_{Ex}) (given by Equation 3.10) would be injected into the battery bank for storage. The battery charge ($P_{B.Ch}$) which would be the power injected into the battery bank could be calculated according to Equation 3.11.

$$P_{Ex}\ (t) = \eta_{inv1} \times P_{pv}\ (t) - P_L\ (t) \qquad 3.10$$

$$P_{B.Ch}\ (t) = \eta_{batt} \times \eta_{inv2} \times (P_{pv}\ (t) - P_L\ (t)/\ \eta_{inv1}) \qquad 3.11$$

where η_{inv1} would be the solar inverter efficiency and P_L would denote the load demand, η_{inv2} would be the inverter charger efficiency and η_{batt} would be the battery charge/discharge efficiency. If P_{Ex} was more than the battery maximum State of Charge, the excess power would be wasted or dumped or used to power a dump load.

B. If $\eta_{inv1} \times P_{pv}\ (t) < P_L\ (t)$, then two states (B.1. and B.2.) might happen. At first, the deficit power (P_d) would be met by the battery bank, which could discharge energy only when its depth of discharge (DOD) was less than the maximum allowed. In this case, the deficit power would be calculated according to Equation 3.12:

$$P_d\ (t) = P_L\ (t) - \eta_{inv1} \times P_{pv}\ (t) \qquad 3.12$$

The required battery bank capacity for meeting all the deficit power was calculated as follows:

$$P_{B\text{-}disch}\,(t) = P_d\,(t) \div (\eta_{inv2} \times \eta_{batt}) \qquad 3.13$$

If $P_L\,(t) > \eta_{inv1} \times P_{pv}\,(t) + P_{B\text{-}disch}\,(t)$, the combined output of the battery bank's capacity and the PV array would not be enough to satisfy the load, the load could therefore entirely be met by running the backup DG system. The required power to be met by the DG system was calculated according to Equation 3.14:

$$Pdg\,(t) = P_L\,(t) - \eta_{inv1} \times P_{pv}\,(t) - P_{B\text{-}disch}\,(t) \times \eta_{inv2} \times \eta_{batt} \qquad 3.14$$

Since the DG system could not generate more electricity than its rated power, if $P_{dg}\,(t) > P_{dgn}$, then $P_{dg}\,(t) = P_{dgn,}$ the loss of power supply was then calculated as follows:

$$LPS\,(t) = PL\,(t) - \eta_{inv} \times P_{pv}\,(t) - P_{dgn} - P_{B\text{-}disch}\,(t) \times \eta_{inv2} \times \eta_{batt} \qquad 3.15$$

where $P_{dg}\,(t)$ is the required DG power and P_{dgn} is the rated DG power.

If $Pdg\,(t) > P_L\,(t)$, the excess power produced by the DG system, which would then be added to the battery bank could be determined by using Equation 3.16.

$$P_{B.Ch}\,(t) = \eta_{batt} \times \eta_{inv2} \times (P_{dgn} - P_L\,(t)) \qquad 3.16$$

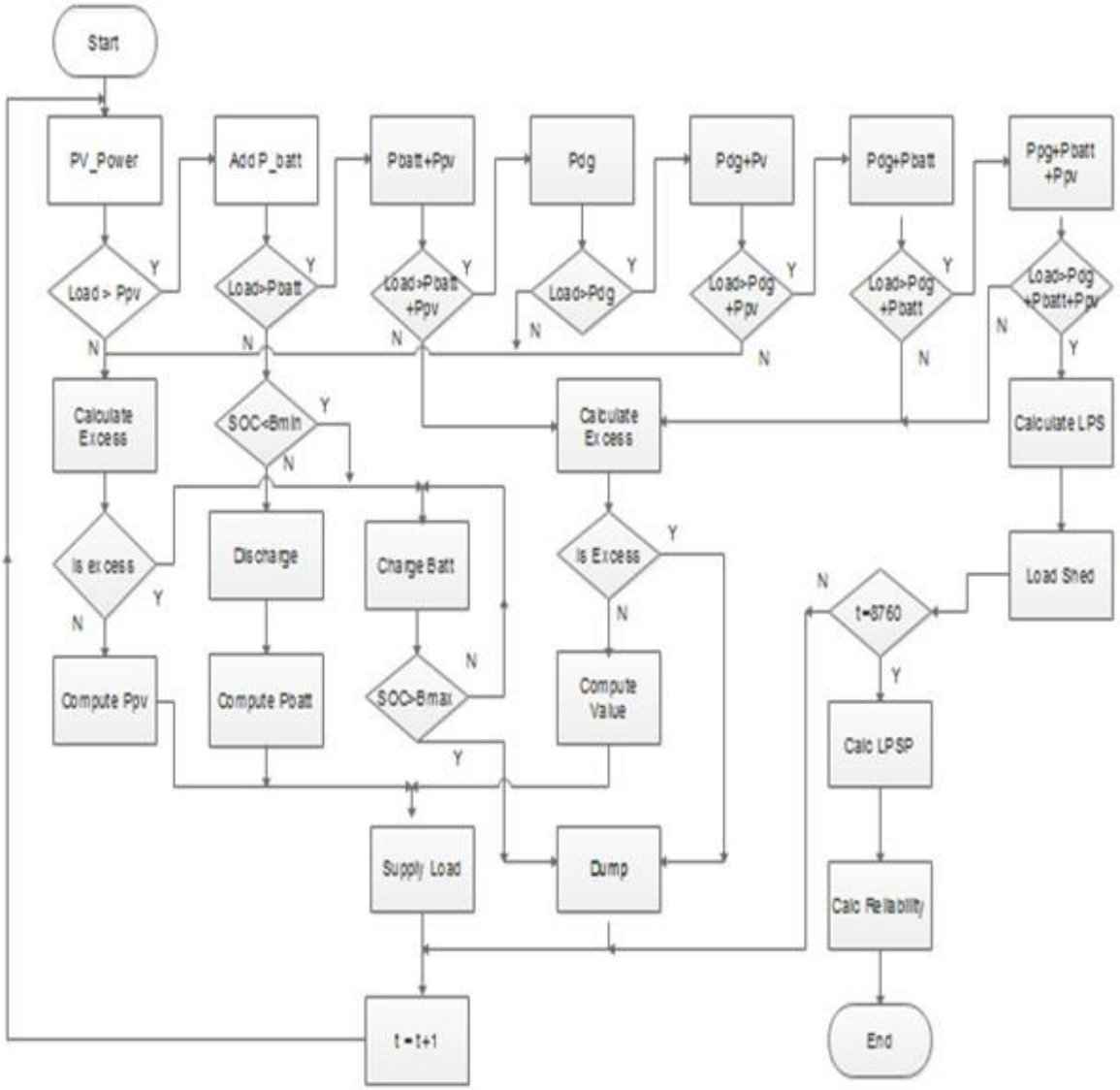

Figure 5 Flowchart of the Energy Management System

3.5 Optimization and Control Strategy

3.5.1 Optimization

The objective function of this study was to determine the minimum unit cost of energy. The optimization method used in this study was that of Hove (2000), i.e. a method for dimensioning a power system by way of simulating the hourly power supply flow and

then matching it to the hourly load profile until the desired level of energy supply reliability is achieved. The optimization was based on the estimated AC load of the village, the hourly profile, the PV array size, the DG rated power, the battery capacity, and the strategy employed for dispatching DG energy. To attain a certain prescribed degree of supply reliability, the chosen combination of component sizes should always be able to deliver enough energy. The supply reliability would be measured by the loss-of-load fraction (LLF, defined by Hove as the fraction of annual hours when the power supply system failed to completely satisfy the load). Hove argued that, in this way, the combination resulting in the Least Energy Cost would be the optimum system.

The hybrid system design space was defined by generating a family of system sizing curves that plot the PV array size required to attain a prescribed LLF, against battery sizes, for different discrete values of DG size. Hove used dimensionless variables to represent the hybrid system component sizes, and therefore, similarly, in this study the PV array size was indicated by the normalized variable ^{P} , where P was the actual
$_{P_0}$
installed PV array power and P_0 was a hypothetical power, conceptualized as the PV array power required for satisfying a daily electrical Load of L_{day} [kWh] if the array was operated at reference efficiency, and reference solar irradiance constantly, throughout the day, such that:

$$P_0 = \frac{L^{day}}{24} \qquad 3.15$$

3.5.2 Dispatch strategy

A dispatch strategy in a hybrid system would be a control algorithm of the switching generator and the battery bank if there was insufficient renewable supply to meet the load demand. For this study, Cyclic Charging (CC), was considered for the hybrid PVDiesel system with (Li-ion) Batteries. In CC strategy, the generator would be run at

its full capacity, and after meeting the load demand, the rest of the generated energy would charge the battery bank. The diesel generator would be switched on only when the battery bank's State of Charge fell below the prescribed value, SOC_{set}.

3.6 Model Inputs

The spreadsheet model, developed as part of this study, used the inputs of the three dimensionless variables $\frac{P}{P_0}$, $\frac{B_{cap}}{L_{day}}$ and $\frac{G_{cap}}{L_{day}}$ as well as the inputs defining the diesel generator strategy to compute the LLF and the Cost of Energy.

3.6.1 Array Input parameters

The input parameters for the array are shown in Table 5 below. The latitude of the site determined the angle of tilt to which the panels should be set. The preferred zenith angle was 180 (north facing) to take full advantage of the year-round radiation. The reference efficiency of the state-of-the-art PV arrays, as well as the temperature coefficient, used in this study, are indicated. The PV power was obtained by inputting the normalized variable $\frac{P}{P_0}$.

Table 5 *Array Input Parameters for the model*

Parameter	Unit	Value
Tilt	° degrees	37°
Azimuth	° degrees	180°
Latitude	Radians	
normalized variable $\frac{P}{P_0}$		Zz
Reference Efficiency	%	18
Temperature	°C	25

3.6.2 Battery Input Parameters

The battery's input parameters are shown in Table 6. The system voltage of the battery was assumed to be 48V. The normalized effective battery capacity was obtained by dividing the daily load into the standard battery capacity, $\frac{B_{cap}}{L_{day}}$.

Table 6 *Array Input Parameters for the model*

Parameter	Unit	Values
$\frac{B_{cap}}{L_{day}}$		Zz
Capacity	kWh	Zz
Allowable DOD	%	20
Roundtrip efficiency	%	95
Battery System Voltage	Volts (V)	48

3.6.3 Diesel generator Input Parameters

The input parameters of the diesel generator are shown in Table 7. The diesel generator capacity was determined by the peak demand of the generic village, with an additional safety margin of 20%. The minimum load factor for the diesel generator to protect it from damage when loads were below a certain threshold was assumed to be 30%. The dimensionless variables $\frac{G_{cap}}{L_{day}}$ that corresponded with standard diesel generator capacity values of 15, 20, 25, 30, and 40 kW were used, to avoid the dangers of oversizing or under-sizing. (It was explained in section 2.11 that, oversizing could reduce the generator's life, as well as increase its fuel consumption rate, as Gensets would run optimally at levels between 50% and 80% of its capacity).

Table 7 Generator input for the model

Parameter	Unit	Values
$\frac{G_{cap}}{L_{day}}$		Xx
Diesel Generator Runtime	Hours	15000
Minimum Load for Generator	%	25
Average Fuel Efficiency	%	20
Maximum Load	kW	Xx
Safety Factor	%	30

3.6.4 Economic Input Parameters

The economic parameters provided to the model included the estimated project capital costs (including the cost of the system components), details of the replacement periods of components, maintenance parameters, project running costs and other economic parameters are shown in Tables 8 to 11. To construct a hybrid off-grid system, the up-front purchases of power production and distribution and metering infrastructure are made. The individual cost components of the hybrid off-grid system were the ongoing costs such as those associated with fuel, operations and maintenance, overheads, losses, and lower capacity utilization. The up-front costs consisted of the Capital expenses (Capex) and the project development and construction costs. Tables 8 to 11 list the assumptions made for economic input parameters.

Table 8 *General inputs*

The modeling assumptions	Unit	Assumption
Lifetime of Investment	Years	20
Target Installed Capacity	kW	200
Number of people to be electrified	Ppl	1546.805912
Average household size	ppl/hh	5.1
Daily household income	USD/hh/day	6.375
The average number of household connections	Hh	303
Effective Corporate Tax Rate	%	0.25
VAT	%	0.15
Import duty	%	0.35

Table 9 Systems and investment cost inputs

INVESTMENT COST	Unit	Assumption
Investment Cost, Generation		
Solar PV	USD/kWp	200
Racking	USD/kWp	40
PV BOS (Includes BOS, AC Station, Comms/ Monitoring system)	USD/kWp	80
Battery	USD/kWh	250
Inverter	USD/kWp	100
Inverter Charger	USD/kWp	180
Mounting Structure, Battery Room, etc.	USD/kWp	10
Back-Up Gen	USD/kWp	200
Project Development $ Construction	% of Investment cost	12
Investment Cost, Distribution		
Low Voltage Distribution Line, Distance	Km	3
Low Voltage Distribution Line, Cost	USD/km	7000
Transformer (25KVA/50kVA)	Units	6
	USD/unit	1700
End-User Equipment	USD/end-user	170
Distribution network lifetime	Years	20
Depreciable base of the initial investment (Solar PV modules)	%	100

Table 10 Operational inputs

The modeling assumptions	Unit	Assumption
Operations & Maintenance Expense, Generation & Distribution		
Solar PV-Battery O&M		
Operations & Maintenance expenses as a % total investment	%	3
Annual Inflation adjustment, starting in year 2	%	4
Diesel Gen		
Operations & Maintenance Expense, excluding fuel, year 1	USD/kWh	0.02
Annual Inflation adjustment, starting in Year 2	%	5%
All-in Fuel Costs	USD/L	1.12
Corporate Overhead Allocation		
All overhead	%	30
Losses and underutilization	%	5.4
Fuel cost	%	17
Maintenance CapEx, Distribution		
Battery Replacement	years	5
Inverter and battery chargers	years	7
Depreciable base for Maintenance CapEx	%	100
Diesel Generator Replacement	Years	6
Diesel Gen CapEx	%	0.7
Battery CapEx	%	5.3
Inverter CapEx	%	2.5
Maintenance CapEx, Distribution		
Transformer lifetime	years	10
Transformer CapEx	%	0.02
Distribution Losses and lower capacity utilization	%	7

Table 11 Capital structure and financing inputs

The modeling assumptions	Unit	Assumption
CAPITAL STRUCTURE		
% Equity	%	100.0%
% Debt	%	0.0%
COST OF CAPITAL		

Cost of Equity	%	8.9
Cost of Debt	%	0

3.7 Model Outputs

The model provided the output of the hourly energy balance of the hybrid system, which was the required PV array power, inverter power, battery energy capacity, and the diesel generator power. The important outputs of the model were the energy supply reliability and the Levelized Cost of Energy.

3.7.1 Reliability determination

Different levels of power supply reliability were achieved by size combinations of PV array and battery capacity as indicated in Figure 7. Clearly, larger battery sizes would be required for a PV area of the same size to achieve higher levels of reliability. The required battery capacity (*Bcap/Lday*) to achieve a given level of reliability generally would reduce with the PV array power (*P/Po*) provided, but minimal reduction happened as the PV array area was increased. As mentioned previously, when assuming the CC strategy, the generator would be running at its full capacity, and after meeting the load demand, the rest of the power from the generator would charge the battery.

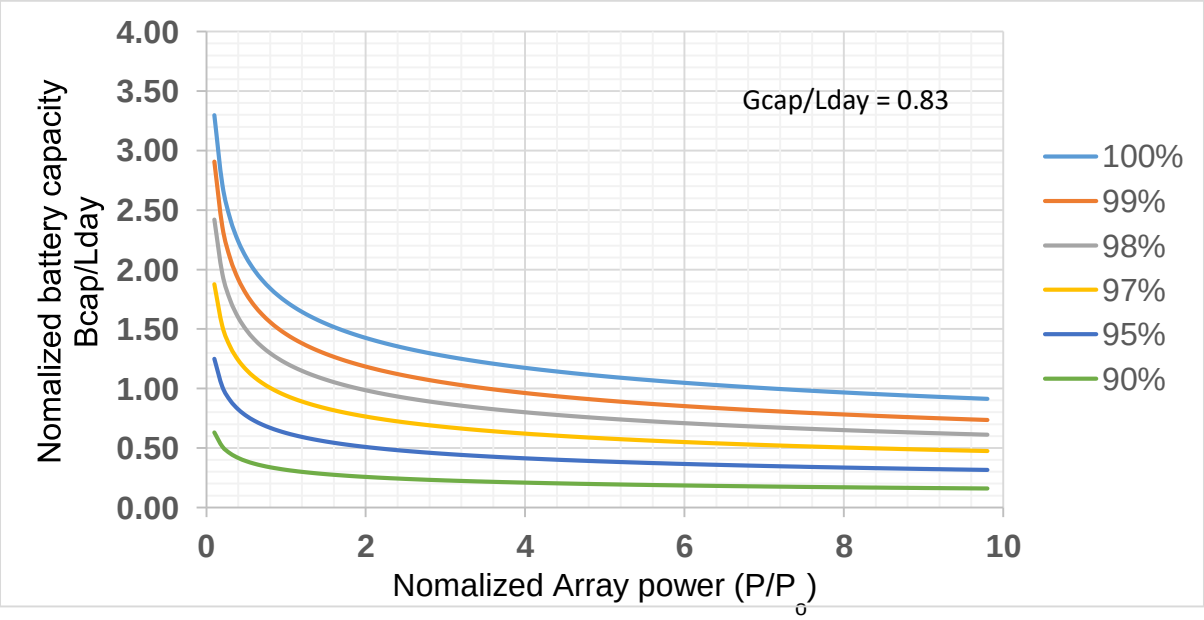

Figure 6 Array area against Battery Capacity

3.7.2 Levelized Cost of Energy (LCOE)

As part of its output the model also provided the LCOE calculated from the different input parameters. The LCOE was the total cost of producing a kilowatt-hour (kWh) of electricity over the lifetime of a project. It was calculated by dividing the total cost over the proposed project life by the estimated amount of electricity generated over the same period, to yield an average cost, expressed in USD per kWh. Equations 2.16 to 2.20 were used for this calculation. The costs comprised the estimated amount of capital investment, the operating and maintenance (O&M) costs, and the replacement costs. Both the costs and the total generation per year were discounted to a reference date using a discounting rate that reflected the cost of capital. Investment (or capital) costs included all expenses incurred before the plant would be operational and any further investments during the life of the plant to maintain or improve its performance levels. These costs would typically involve the engineering, procurement, and construction (EPC) costs; infrastructure and connection costs; development costs including statutory services,, contracted advisory services, acquisition of premises or land; energy resource assessments; insurance, and contingencies. Tax-deductible linear depreciation of 100% of fixed assets over the lifetime of the investment was used. The effective corporate tax rate of Lesotho was 25%, and this figure was used as the tax rate in the model. The relationship of the calculated value of the LCOE and the dimensionless array power generated is shown in Figure 8 below.

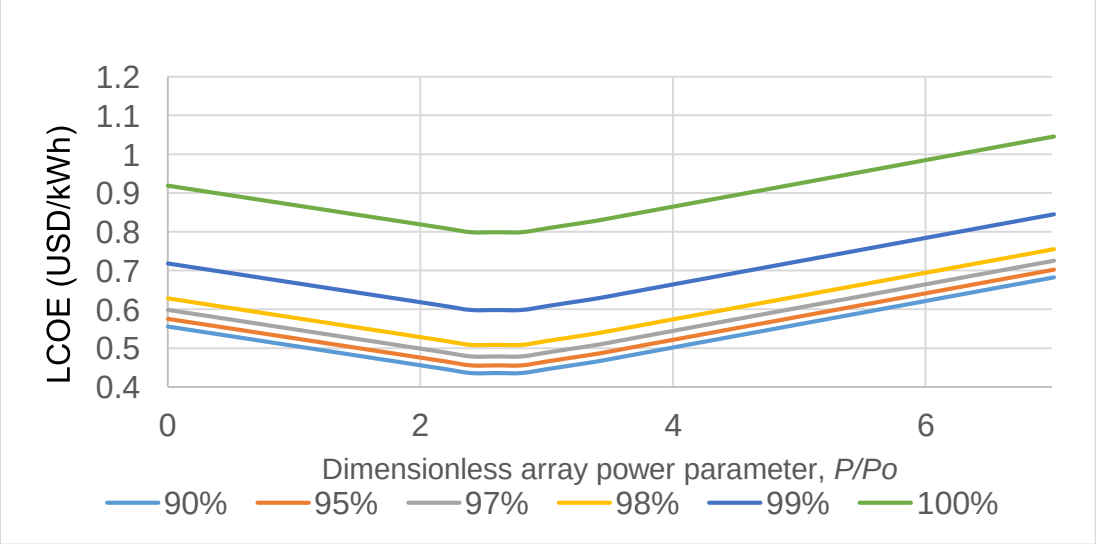

Figure 7 Relationship of LCOE with required dimensionless Array Power (P/Po)

3.7.3 Model Output Visualizations

The model also calculated and displayed the hourly variation of solar power supplied, diesel generator energy supplied, battery charging energy, battery discharge, PV energy dumped, and the load profile, (for three selected consecutive days), for systems achieving any level of reliability. This allows the reader to observe the load demand, the charging cycle of the batteries, the hourly profiles of the solar array power-load, and the levels of reliability throughout all hours of the day, as shown in Figure 9.

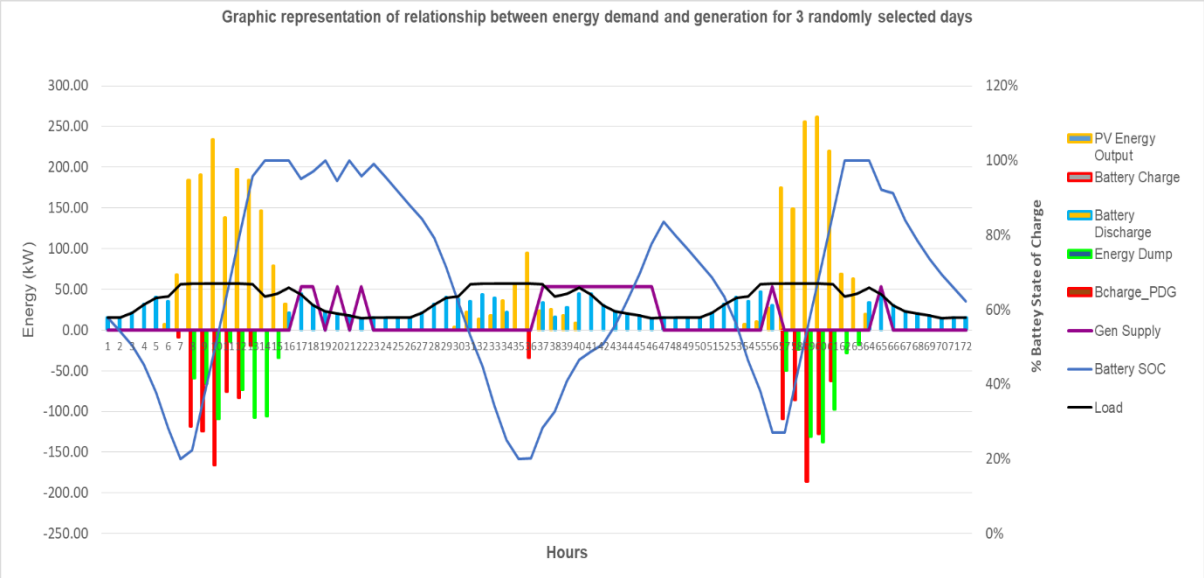

Figure 8 System Performance Visualizations

3.8 Design Selection Criterion

Modeling, simulation, and optimization analyses were performed to determine the energy production from the proposed power system. Three configurations were examined through the simulations. The first configuration was a fossil-fuel system (Diesel only), the second was a Solar PV and Battery Storage (PV-Battery) and, the third one was the Solar PV and Battery Storage in combination with the Diesel generator (PV-Diesel-Battery). In the case of those systems which comprised the diesel generator, the Cycle Charging (CC) control strategy was selected. The best configuration was selected, (i.e. the one which gave the lowest cost of energy at 100

% supply reliability), and thereafter the different combinations of system elements were analyzed to find the one that would be the “best fit”, capable of meeting the energy demands at the least cost.

The LCOE was used as the objective function to select among systems obtaining the same level of reliability as indicated by Figure 6, such that the system with least LCOE that achieved a given level of supply reliability was selected. Based on the information contained in Table 12, a decision could be made about a system to select which would meet the required level of reliability, and the corresponding Levelized Cost of Energy of that system.

Table 12 Decision Matrix for the selection of desired reliability at least levelized cost (PV -Battery)

Reliability	USD/kW	Bcap/ Lday	P/Po	Gcap/Lday
100%	Xx	Zz	Yy	Vv
99%	Xx	Zz	Yy	Vv
97%	Xx	Zz	Yy	Vv
95%	Xx	Zz	Yy	Vv
94%	Xx	Zz	Yy	Vv
92%	Xx	Zz	Yy	Vv
90%	Xx	Zz	Yy	Vv

3.9 Marginal Return Curves

Figure 10 shows by using a graph, the relationship of various values of the LCOE against Reliability for a PV-Battery system and indicates the optimum point at which a system meets the constraints at the minimum cost. This is a curve that represents all minimum cost values for different reliability options. These are the points at which optimal benefits (high reliability or solar fraction) could be derived from the power system at the least cost. The system combination was found at the point on this curve, which gave the minimum cost at the required reliability. Engineering intuition suggested that the values at the elbow of the graph for each reliability level be taken as the optimum design parameters. As illustrated in Figure 10, the configuration of the system with a 100 % supply reliability level, could be twice the size of the system of

99% supply reliability, as, just by increasing the supply reliability by 1 %, the cost increases disproportionately.

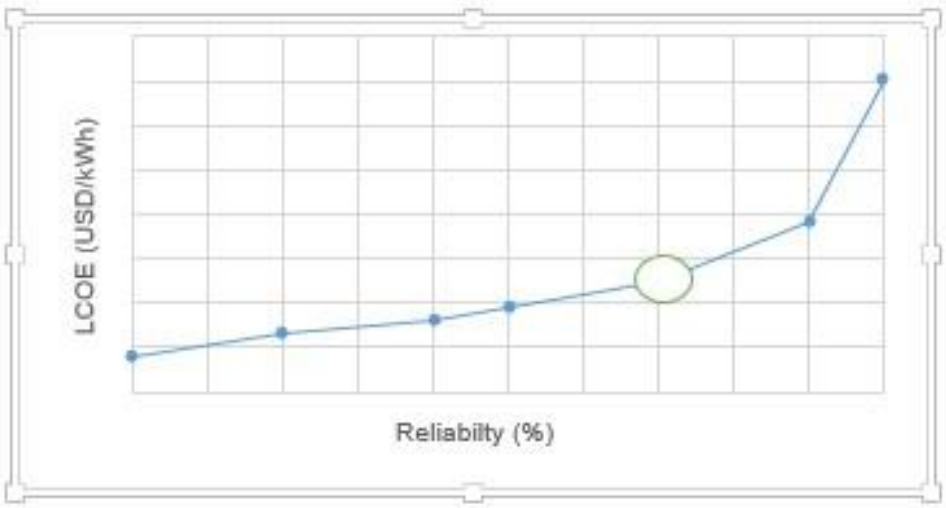

Figure 9 LCOE Vs Reliability Curve PV-Battery System

3.10 System Sizing Calculations

The model used the dimensionless parameters to calculate the actual system components sizes for the required PV array power, the battery capacity, and the Diesel generator power.

3.10.1 PV Array size

Given the daily load L_{day} (Wh), and the required reliability PV array size was obtained as:

$$P_{array} = {}_{P0}\overline{\times}_{24}\frac{P \quad L^{day}}{} \qquad 3.16$$

where, P_{array} is the PV array size, ${}_{P}\_^{P_0}$ is the dimensionless parameter and L_{day} was the daily load.

3.10.2 Battery Sizing

The dimensionless battery size parameter, B_{cap}/L_{day}, which was equal to the ratio of battery energy capacity, B_{cap} [Wh], to the stated daily load, L_{day} [Wh] was used to calculate the actual required battery size:

$$B_{cap} = L_{\frac{B_{cap}}{day}} \times L_{day} \quad 3.17$$

3.10.3 Diesel Generator Sizing

Likewise, the dimensionless diesel generator size parameter, B_{cap}/L_{day}, which was also equal to the ratio of diesel generator power, G_{cap} (W), to the stated daily load, L_{day} [Wh] was used to calculate the actual required diesel generator size:

$$G_{cap} = {}_{L}\overline{G_{day^{cap}}} \times \overline{L_{day}}_{24} \quad 3.18$$

3.10.4 Components and Size of the Hybrid Power System

Table 13 lists the components of the proposed hybrid power system and their specifications, such as solar PV system, diesel backup generator, battery bank, solar inverter, and charger inverter.

Table 13 System components and specifications

System Component	**Description**

Solar Photovoltaic	Solar PV module: polycrystalline, nominal maximum Rated power = 340 W, efficiency = 17.97%, derating factor DF = 91.2%, The life time is 25 years.
Backup Generator	Maximum Power (Capacity PBG)max = 54 kW, Fuel = Diesel, efficiency (η) = 30%, calorific value of diesel (kJ/kg) = 44,800, density of diesel (kg/L) = 0.832, Minimum Load Ratio = 30%, Generator life time (hours) = 15,000.
Battery	Edison, LFP700Ah, Lithium Nominal voltage = 48 V, Battery with a capacity of 700 Ah Battery lifetime = 6 years Minimum SOC = 20% Discharge / Charge efficiency = 95%
Solar Inverter	SMA, String, 25550 Wp, 60 Hz Nominal power 25.55 kW Max.DC Input Voltage = 1000 V AC power frequency/range - 50 Hz / 45 Hz to 55 Hz Lifetime 9 years
Charger Inverter	SMA,Sunny Island, 8000 Wp, 60 Hz DC Nominal power = 8kW Nominal.Input Voltage = 48 V Rated DC charging current = 115 A DC discharging current = 130 A Max.Efficiency = 96 % Lifetime = 7

3.11 Sensitivity analysis

Most of the operational input parameters to the model were beyond our control. Sensitivity analyses was performed. The objective of the sensitivity analyses was to

gain a better understanding of the robustness of the outputs and to be able to test different scenarios. A sensitivity analysis had been performed for the following input parameters: the fuel cost, discount rate, costs of overall capital, PV modules, and battery bank the fuel cost, Discount rate, costs of overall capital, PV modules, and battery bank. The sensitivity analyses illustrated the degree to which each input parameter affected the outputs. In each case, all other assumptions have been constant.

Chapter 4: Results

This section provides the results obtained for the photovoltaic generator power output modeling, the meteorological data, the system components modeling, system performance analysis, and design selection conditions.

Based on the electricity demand profile for the generic village studied, the power generation capacity of the baseline diesel generator mini-grid and the renewable technology, solar PV-battery mini-grid were modeled. Using the spreadsheet model, the solar PV and battery sizes were optimized for the lowest LCOE, provided that the service level did not fall below the required supply reliability.

The modeling, simulation, and optimization results of the proposed renewable power systems are presented here. The results include the daily and yearly performance (production or supply and consumption or demand) of the hybrid power system over the system's projected life. The proposed power system was designed to serve a typical rural village with an estimated load demand of 879 kWh/day, and the best configuration is shown in Figure 11. It was assumed that the hybrid mini-grid system would generate electricity to serve a total number of 250 households, 19 businesses, and 16 institutions situated in the Ribaneng village (latitude: 29.8442° S, longitude: 27.6627° E) in Mohale's Hoek District, Lesotho.

Modeling, simulation, and optimization analysis were performed to determine the energy production from the power system. Three configurations were analyzed by the simulations. The first configuration was a fossil fuel system (Diesel only), the second was a Solar PV and Battery storage (PV-Battery) and a third one was Solar PV and battery storage in combination with Diesel generator (PV-Diesel-Battery). In the case of systems comprising diesel generators, the Cycle Charging (CC) control strategy was selected. The best configuration design was selected, which would give the Lowest Cost of Energy at 100 % supply reliability, and different combinations of system elements were analyzed to get the "best fit" capable of meeting the energy demands at the least cost.

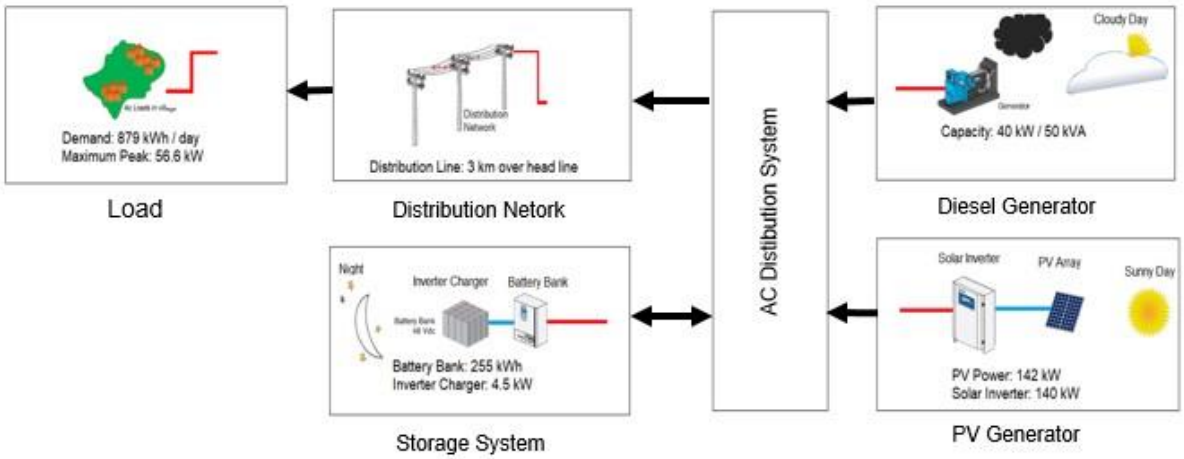

Figure 10 Block diagram of PV-Diesel Hybrid system with storage (PV-Diesel-Battery Configuration)

4.1 Meteorological data

Renewable Resources

The study considered a typical village, remotely located in the southern part of Lesotho, in the Mohale's Hoek district (latitude: 29.8442° S, longitude: 27.6627° E). The proposed study area was not connected to the national electricity grid and kerosene, candles, and biomass were the sources of lighting and cooking. Figure 12 contains the monthly solar irradiation and clearness index data. The average solar irradiation of the selected area was 5.3 kWh/m^2/day (158.2 kWh/m^2/month) and the area has a clearness index of 0.64. The average ambient temperature was 12.7 ˚C. As shown in Figure 13, the model predicted average tilted irradiation of 29.17 (kWh/m2/month) per month.

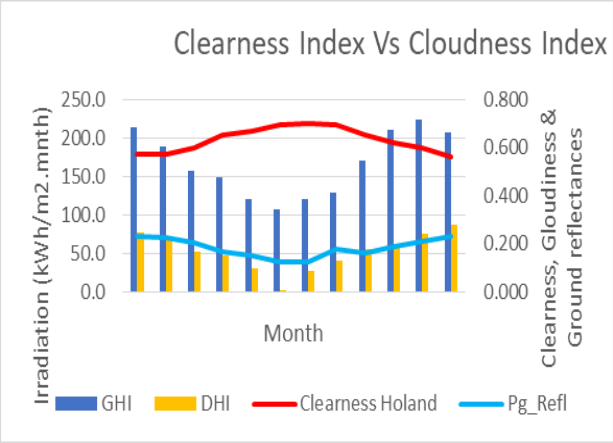

Figure 112 Model monthly average irradiation & clearness

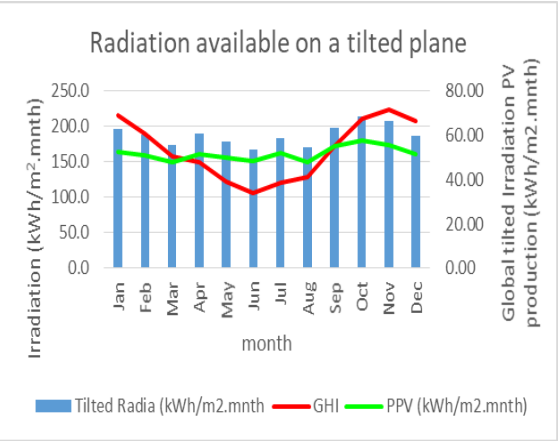

Figure 123 Model monthly radiation available on tilted plane

4.1 System Components modeling

4.1.1 Photovoltaic Generator Power Output Modeling

The values produced by the Photovoltaic Generator Power Output Modeling process are shown in Table 14, 15, and 16. The evaluation of the hourly variation of efficiency and the calculation of the corresponding hourly-average PV module power output were performed. An extract of TMY data for the location (latitude: 29.8442° S, longitude: 27.6627° E) is shown in Table 14 below. Other meteorological variables important for the PV output analysis (such as ambient temperature, the hourly meteorological values G_h (global horizontal irradiance) and G_d (diffuse horizontal irradiance)) are also shown in the TMY data. The power from the solar photovoltaics decreases at high temperature and also with the accumulation of dust or sand on the solar panels. The effect of the soiling on the power produced from the solar PV was included in the calculation of the derating factor (DR) shown in Table 16.

Table

14 Sample of Typical Meteorological Year Data for a place

Dry bulb temperature (deg. C)	Relative Humidity (%)	Global horizontal irradiance (W/m2)	Direct (beam) normal Irradiance (W/m2)	Diffuse horizontal irradiance (W/m2)	Infrared radiation downwards (W/m2)	Windspeed (m/s)	Wind direction (deg.)	Air pressure (Pa)	Day Number
14.26	81.36	0	0	0	349.5	1.58	94	78098	1
14.43	80.77	0	0	0	348.37	1.43	90	78105	1
14.59	80.19	0	0	0	347.25	1.28	86	78113	1
14.75	79.6	0	0	0	346.12	1.13	93	78139	1
14.92	79.02	17	0	17	344.99	0.99	100	78164	1
15.08	78.43	166	20.82	158	343.87	0.84	106	78190	1
15.25	77.85	485.95	574.61	153	342.74	0.69	126	78149	1
15.41	77.26	482	122.98	390	341.61	0.54	145	78108	1

Table 15 Process for predicting hourly irradiation on the tilted surface

Hour	delta (δ)	omega (ω)	cosθz	cosθ	Rb	Ib	Ib*Rb	Fc-sky	Fc-ground	Ai	Hottel & Woertz 1942	Liu and Jordan (1963)	Hay and Davies	Temps & Couson	HDKR Model
0.00	-0.40	-2.51	-0.46	-0.75	0.00	0.00	0.00	0.93	0.07	0.00	0.00	0.00	0.00	0.00	0.00
1.00	-0.40	-2.30	-0.35	-0.62	0.00	0.00	0.00	0.93	0.07	0.00	0.00	0.00	0.00	0.00	0.00
2.00	-0.40	-2.09	-0.21	-0.47	0.00	0.00	0.00	0.93	0.07	0.00	0.00	0.00	0.00	0.00	0.00
3.00	-0.40	-1.88	-0.06	-0.29	0.00	0.00	0.00	0.93	0.07	0.00	0.00	0.00	0.00	0.00	0.00
4.00	-0.40	-1.68	0.11	-0.10	0.00	0.00	0.00	0.93	0.07	0.00	0.00	0.00	0.00	0.00	0.00
5.00	-0.40	-1.47	0.28	0.09	0.00	0.00	0.00	0.93	0.07	0.00	0.00	0.00	0.00	0.00	0.00
6.00	-0.40	-1.26	0.44	0.28	0.00	0.00	0.00	0.93	0.07	0.00	17.00	16.54	16.54	16.82	16.54
7.00	-0.40	-1.05	0.59	0.46	0.33	8.00	2.66	0.93	0.07	0.05	160.66	156.74	152.17	154.60	152.70
8.00	-0.40	-0.84	0.73	0.61	0.64	332.95	211.85	0.93	0.07	0.69	364.85	374.13	343.03	343.81	343.67
9.00	-0.40	-0.63	0.84	0.74	0.77	92.00	70.68	0.93	0.07	0.19	460.68	453.93	441.66	446.77	443.90
10.00	-0.40	-0.42	0.92	0.84	0.84	679.80	570.19	0.93	0.07	0.79	750.24	772.74	759.32	759.93	759.86
11.00	-0.40	-0.21	0.98	0.90	0.88	132.00	116.14	0.93	0.07	0.20	633.14	624.59	619.00	625.67	622.01
12.00	-0.40	0.00	0.99	0.92	0.90	0.00	0.00	0.93	0.07	0.00	163.00	158.63	158.63	161.27	158.63
13.00	-0.40	0.21	0.98	0.90	0.92	0.00	0.00	0.93	0.07	0.00	252.00	245.25	245.25	249.32	245.25
14.00	-0.40	0.42	0.92	0.84	0.92	0.00	0.00	0.93	0.07	0.00	199.00	193.67	193.67	196.89	193.67
15.00	-0.40	0.63	0.84	0.74	0.92	0.00	0.00	0.93	0.07	0.00	144.00	140.14	140.14	142.47	140.14

Table

16 Photovoltaic Generator Power Output Model

Hour	Dry bulb temperature (deg. C)	Temperature Cell	ηPV	ηPV/ηSTC	Gtilted/Gstc	P_{PV}	P_{pv} (after losses)
0	11.1	0.000	0.167	0.838	0.000	0.000	0.000
1	11.41	0.000	0.167	0.838	0.000	0.000	0.000
2	11.73	0.000	0.167	0.838	0.000	0.000	0.000
3	12.04	0.000	0.167	0.838	0.000	0.000	0.000
4	12.35	0.000	0.167	0.838	0.000	0.000	0.000
5	12.67	0.000	0.167	0.838	0.000	0.000	0.000
6	12.98	20.499	0.165	0.846	0.083	12966.704	11942.335
7	13.3	21.935	0.164	0.852	0.136	21323.659	19639.090
8	17.43	29.829	0.158	0.888	0.465	75973.633	69971.716

4.1.2 Battery Bank (BB) Modeling

The results obtained from using the Excel spreadsheet model for the battery storage are shown in Table 17. Important information such as the battery state, the battery State of Charge, and the Cycle Count are also shown. The model calculated the availability of the battery and indicated its State of Charge. It also computed whether there would be residual demand present during the last hour. It concluded that there would be no diesel generation in the last hour and that there would be energy in the battery. If there was enough energy left in the battery, the model could also opt to use it to meet the residual demand of the past hour, but if there was not enough energy, it would chose to use the generator to meet the demand and to charge the battery.

Table

17 Battery bank spreadsheet modeling results

Hour	Battery state	Bcharge_ P_{Pv}	Bch_Plot	Battery discharge	Bsoc	Charge(1) / discharge(0)	Cycle Count	DoD of cycle
1	258.57	0.00	0.00	15.61	95%	0	0	0.00
2	242.28	0.00	0.00	15.61	89%	0	0	0.00
3	225.99	0.00	0.00	15.61	83%	0	0	0.00
4	209.69	0.00	0.00	15.61	77%	0	0	0.00
5	193.40	0.00	0.00	21.52	71%	0	0	0.00
6	170.94	0.00	0.00	31.85	63%	0	0	0.00
7	137.70	0.00	0.00	28.94	51%	0	0	0.00
8	107.74	0.00	0.00	22.29	40%	0	0	0.00
9	84.89	2.93	(2.93)	0.00	31%	0	0	0.00
10	88.95	21.12	(21.12)	0.00	33%	1	1	0.67
11	111.38	45.95	(45.95)	0.00	41%	1	0	0.00
12	158.89	58.10	(58.10)	0.00	58%	1	0	0.00
13	212.64	59.92	(59.92)	0.00	78%	1	0	0.00
14	266.39	6.17	(6.17)	0.00	98%	1	0	0.00
15	272.56	0.00	0.00	0.00	100%	1	0	0.00
16	272.56	0.00	0.00	0.00	100%	0	0	0.00
17	272.56	0.00	0.00	1.06	100%	0	0	0.00
18	272.39	0.00	0.00	45.62	100%	0	0	0.00

4.1.3 Diesel generator modeling

As explained in Section 4.1.2, the model simulated the use of the generator to meet the specified demand and to charge the battery if the energy in the battery was not enough to meet demand. Table 18 shows the results obtained from the diesel generator modeling process: i.e. the model's prediction of the amount of fuel to be used for every hour, the excess energy that would be dumped, and the capacity of diesel energy that would be required to service the load demand.

Table

Table 18 Diesel generator spreadsheet modeling

Hour	Gen Status ON =1 OFF = 0	Diesel generation (kWh)	Fuel consumption (L)	Dumped
1	1	48.36	15.57	32.90
2	1	48.36	15.57	32.90
3	1	48.36	15.57	32.90
4	0	0.00	0.00	0.00
5	1	48.36	15.57	27.05
6	0	0.00	0.00	0.00
7	1	48.36	15.57	8.56
8	1	48.36	15.57	6.96
9	1	48.36	15.57	0.00
10	1	48.36	15.57	0.00
11	0	0.00	0.00	0.00
12	1	48.36	15.57	0.00
13	1	48.36	15.57	0.00
14	0	0.00	0.00	0.00
15	1	48.36	15.57	0.00
16	1	48.36	15.57	7.54
17	0	0.00	0.00	0.00

As explained, the modelling was done to assess whether enough energy would always be made available for the demand since a cost-efficient design of a hybrid powersystem must match the production capacity to the local demand. Therefore, the demand should be properly predicted. To predict the load more precisely it was necessary to have an understanding of both the maximum load as well as the impact pattern of that load. The next section shows the results obtained from the process of load prediction.

4.3 Load profile

This study's subject was a rural community of approximately 250 households where the daily electricity load demand was estimated to be 879 kWh and the peak load demand approximately 56.6 kW. This electricity load profile was then scaled to the daily demand of 879 kWh. As an hourly time series of radiation data was used, it was

possible to estimate the hourly load profiles (see Figure 14), for the appropriate sizing of the system. As mentioned in previous sections, the usage of the electricity was grouped as Domestic Uses, Productive Uses, and Public Uses. The demand matrix indicated that the individual demands for Domestic Uses, Productive Uses, and Public Uses were 279.98, 252.36, and 235.74 kWh/day respectively. The corresponding maximum peak demands were 17.4, 25.77, and 12.25 for Domestic Uses, Productive Uses, and Public Uses respectively. Figure 15 (Public Uses)shows by way of a piediagram, the individual shares of the various components comprised in the Public Uses group, e.g. schools, churches, and offices, The highest share was that of the communication tower (52 %), which could become an anchor customer. Figure 16 (Productive Uses) shows that, of the Productive Uses, the highest share would be that of the bakery (28 %), and that the bakery could also be made an anchor customer. Figure 17 (Domestic Uses) shows the shares of the domestic users by load type (Low, Medium, Middle, and High).

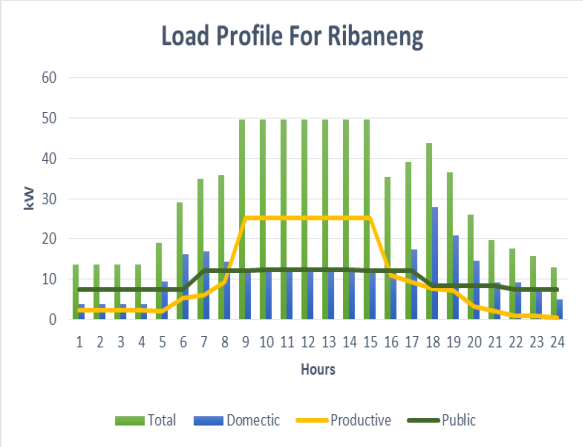

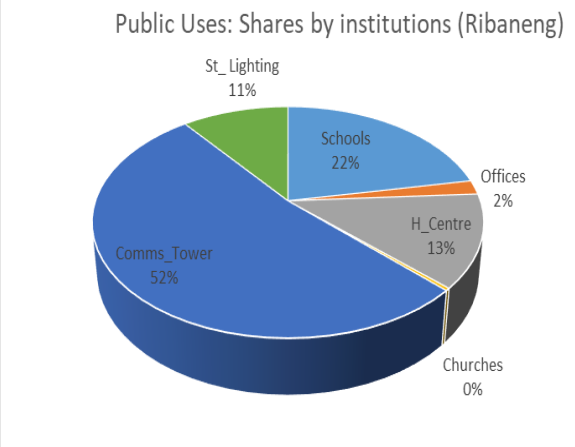

Figure 18 Public uses load demand Figure 15 Load profile prediction of share prediction Ribaneng

Figure 16 Productive uses load share

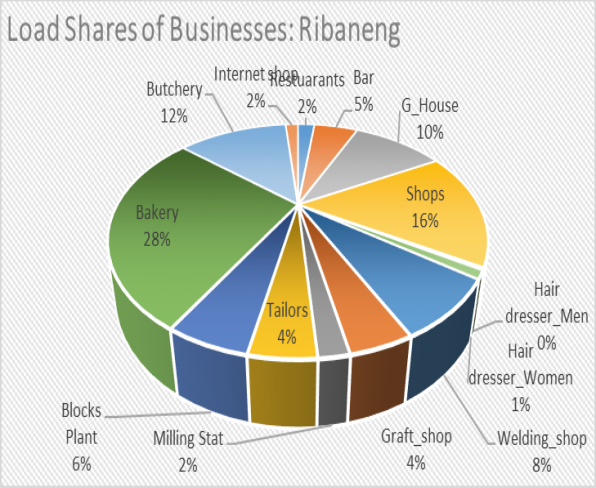

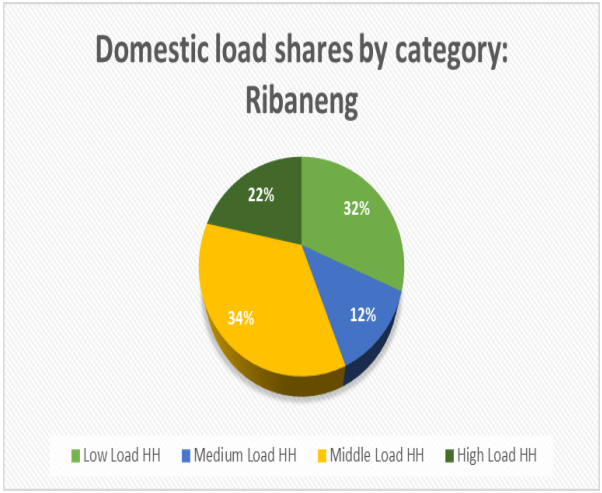

Figure 21 Productive uses load share prediction

Figure 19 Domestic uses load share prediction

The predicted load profile would be supplied by the different technologies in the Hybrid mini-grid system. As explained in previous sections, it would be important to manage the combination of the technologies correctly to maximize the performance of the system and to minimize its costs. Therefore the best system configuration was selected, which would achieve the lowest cost of energy at 100% supply reliability. Details of this configuration are presented in the next section.

4.4 System configuration selection

The configuration of the selected hybridized system consisted of a diesel generator, a PV generator, and a battery bank. For all the combinations that were obtained from the three configurations studied, at 100% supply reliability, the best costs were 0.76, 0.73, and 0.49 USD/kWh for the Diesel only, the PV-Battery and the PV-Diesel-Battery system configurations respectively. The cost, lifetime, and other technical characteristics related to the hardware components in this analysis are presented in Table 19. Table 19 also summarizes the energy production, consumption, excess energy, and the unmet load for the three systems. The Diesel-only system configuration was the most costly. Of the three configurations considered, the PVDiesel-Battery configuration was finally selected.

Table 20 Optimisation summary results of Diesel only, PVBattery & PV-Diesel-Battery systems

Characteristics	**Diesel only**	**PV-Battery**	**PV-DieselBattery**
COE (USD/kWh)	0.76	0.73	0.49
NPC (USD)	2,723,326	1,479,388	1,042,560
Diesel generator (kW)	40	0	40
PV Module (kW)	0	593	593
Battery (kWh)	0	1758	703
Inverter (kW)	0	582	582
Inverter Charger (kW)	0	29	11.61
Excess Energy (kWh/yr)	175,684	779	784
Unment Load (kWh/yr)	0	0	0
Renewable Fraction (%)	0	100%	98.60%
Diesel Gen energy (kWh/yr)	595,546	0	4,497
PV energy (kWh/yr)	0	1112	1117
Fuel Consumption (L/yr)	191,732	0	1447.00

4.5 System configuration performance

Figure 18 shows a comparison between the three configurations for the total energy production from the Diesel only, PV-Battery and PV-Diesel-Battery systems. It shows that the highest energy-producing system would be the Diesel-only, but it would be the most wasteful, as it would always supply its peak energy, even during lower loaddemand situations. The lowest cost producer would be the PV-Diesel-Battery system, as it was sized to supply only the required demand. The PV-Battery system, although it would be the highest in renewable energy fraction, would supply less electricity due to the sizing limitations.

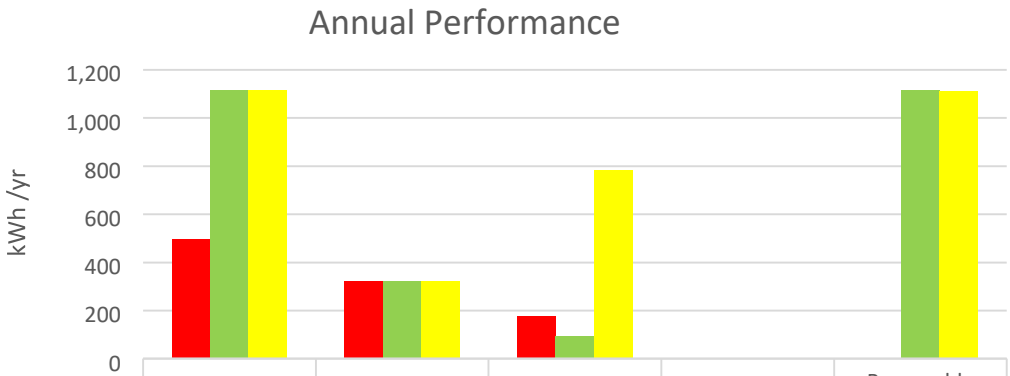

	Production	Consumption	Excess Energy	Unment Load	Renewable Energy
Diesel only	496,588	320904	175,684	0	0
PV-Battery	1,117,382.83	320904	92182	0	1,117,382.83
PV-Diesel-Battery	1,117,382.83	320904	783983	0	1,112,885.56

Figure 24 Yearly performance of the grid hybrid system

To get the best system combination that would be a suitable fit, capable of meeting the electricity demands at the least cost, the PV-Diesel-Battery system configuration that was selected was further analyzed, and an optimum combination was determined: a specific combination (a diesel generator of a suitable size, a battery of appropriate capacity and a solar array of a specific size) which would result in achieving the lowest LCOE. The next section provides the results of the design selection.

4.6 Design Selection

The design space solution systems were dimensioned by way of simulating the hourly power supply flows and matching it to the hourly load profile until the desired level of energy supply reliability was achieved as explained in the methodology section. The design selection was performed by first generating a family of system sizing curves that plotted the PV array size required to attain the prescribed reliability, against

battery size, for different values of diesel generator size. The generator values used were the standard values of 15, 20, 25, 30, and 40 kW, which corresponded to the dimensionless variables of 0.83, 1.1, 1.38, 1.68, and 2.2 respectively. Different levels of power supply reliability were achieved by the size combinations as shown in Figure 19. The internationally recognized supply reliability is 95%. This study dealt with supply reliability ranging from 90 % to 100 %, as it was considered to be a good range for the analyses, given that some power utility companies in Africa provided even less than

90%. Figure 19 shows all possible combinations of components' size variables $\frac{P}{P_O}$, $\frac{B_{cap}}{L_{day}}$ and $\frac{G_{cap}}{L_{day}}$ that satisfied the given load and diurnal profiles of reliability between 90% and 100%. Engineering Intuition Values (at the elbow of the graph) for each reliability were taken as the optimum design parameters. Figure 19 shows sizing curves which represent all components size variables $\frac{P}{P_O}$, $\frac{B_{cap}}{L_{day}}$ with a) $\frac{G_{cap}}{L_{day}}$ = 0.83, b) $\frac{G_{cap}}{L_{day}}$ = 1.1, c) $\frac{G_{cap}}{L_{day}}$ = 1.38, d) $\frac{G_{cap}}{L_{day}}$ = 1.68, and e) $\frac{G_{cap}}{L_{day}}$ = 2.2.

a)

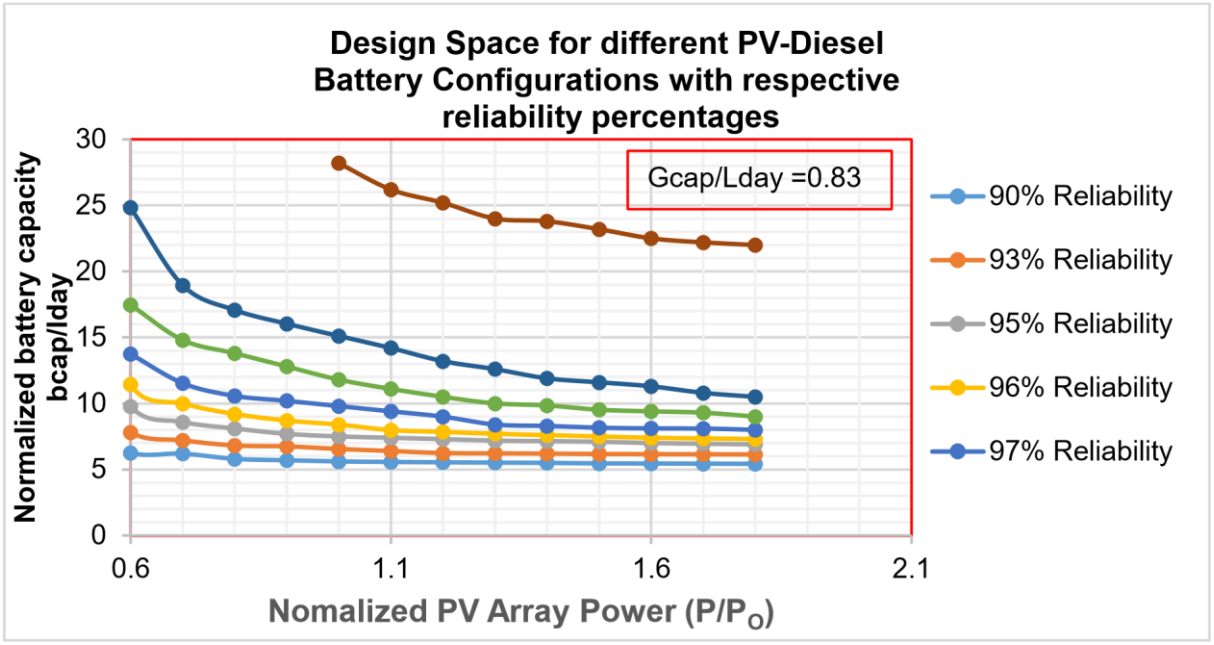

b)

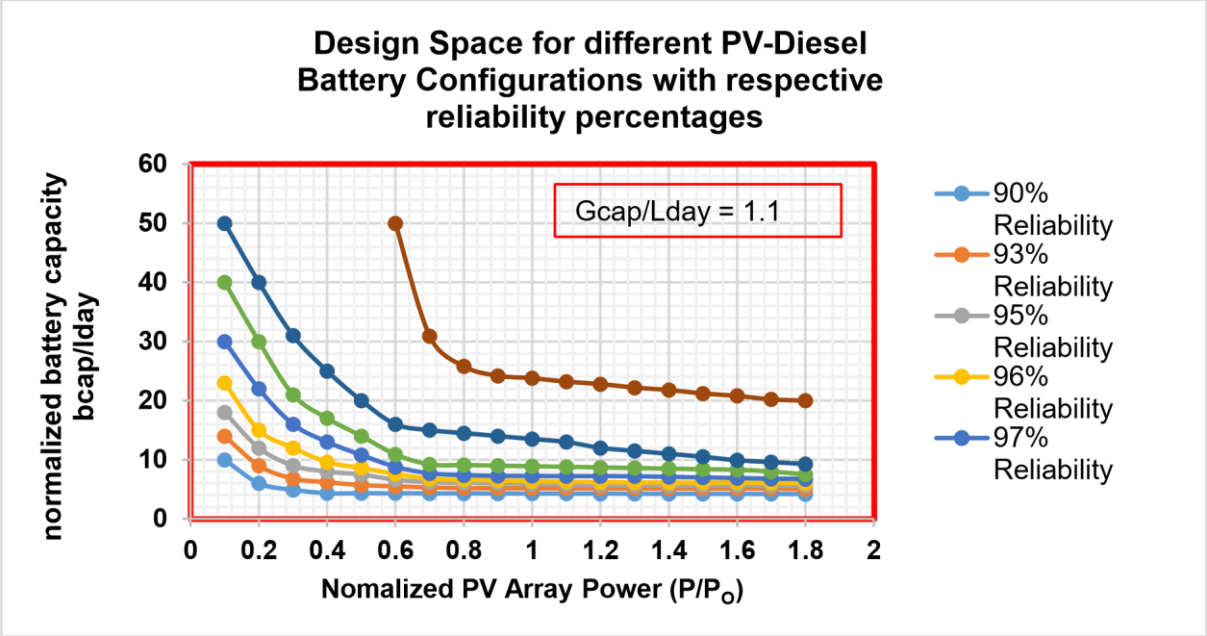
Design Space for different PV-Diesel Battery Configurations with respective reliability percentages
normalized battery capacity bcap/lday
Gcap/Lday = 1.1
Nomalized PV Array Power (P/Po)
90% Reliability
93% Reliability
95% Reliability
96% Reliability
97% Reliability

c)

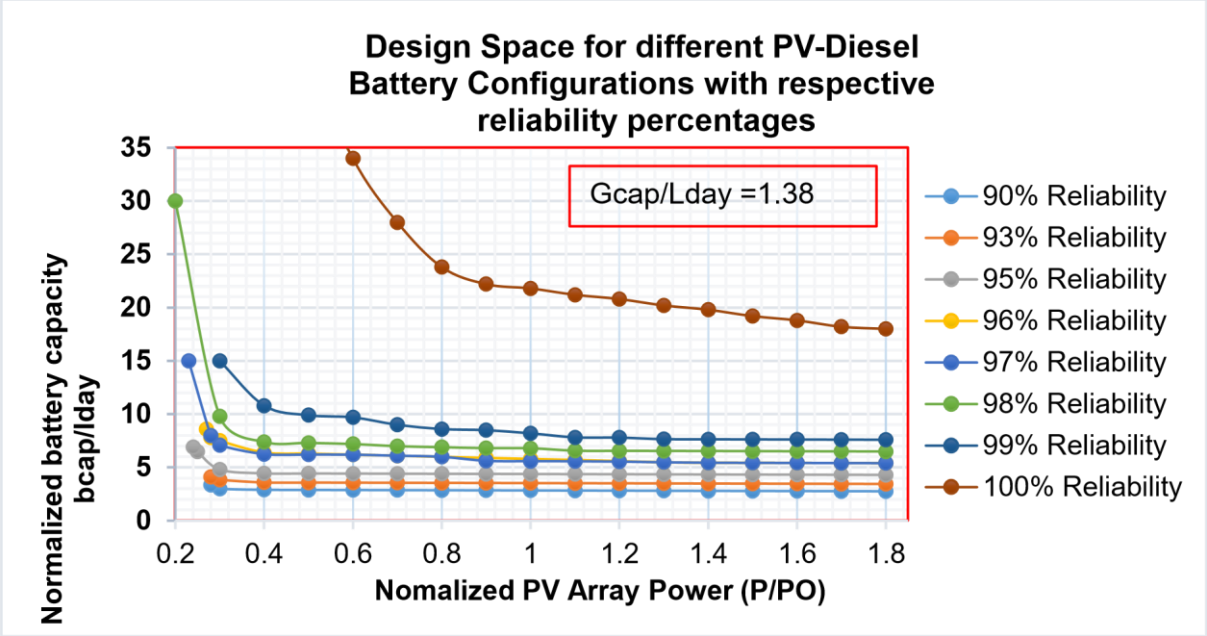
Design Space for different PV-Diesel Battery Configurations with respective reliability percentages
Gcap/Lday =1.38
Normalized battery capacity bcap/lday
Nomalized PV Array Power (P/PO)
90% Reliability
93% Reliability
95% Reliability
96% Reliability
97% Reliability
98% Reliability
99% Reliability
100% Reliability

d)

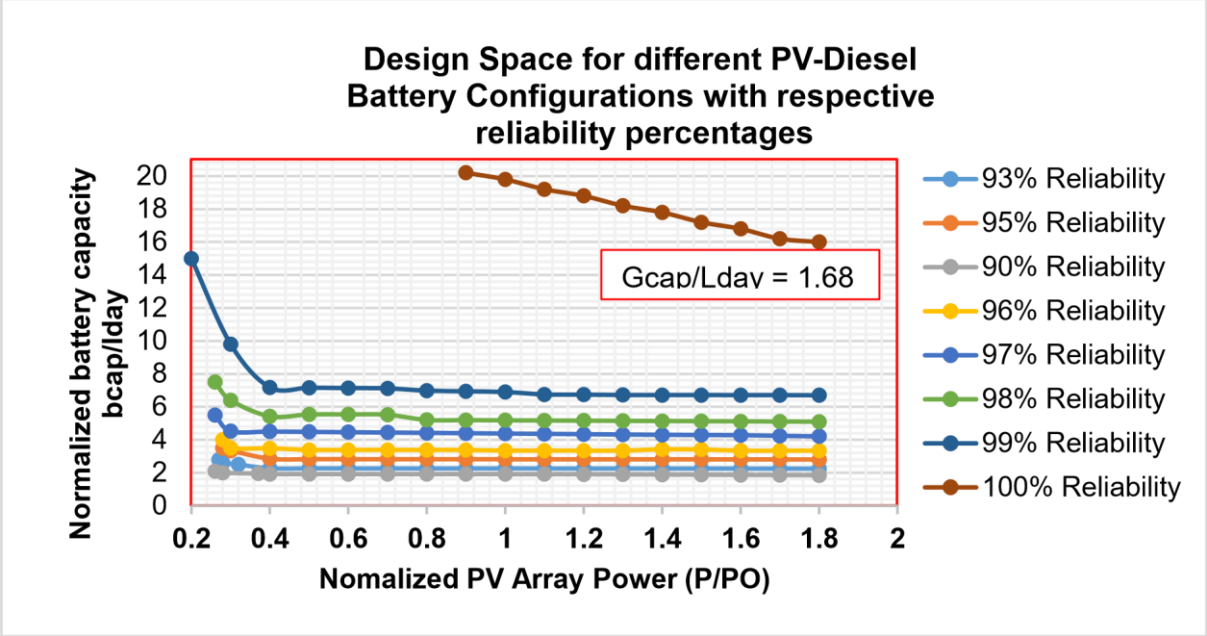
Design Space for different PV-Diesel Battery Configurations with respective reliability percentages
Gcap/Lday = 1.68
Normalized battery capacity bcap/lday
Nomalized PV Array Power (P/PO)
93% Reliability
95% Reliability
90% Reliability
96% Reliability
97% Reliability
98% Reliability
99% Reliability
100% Reliability

e)

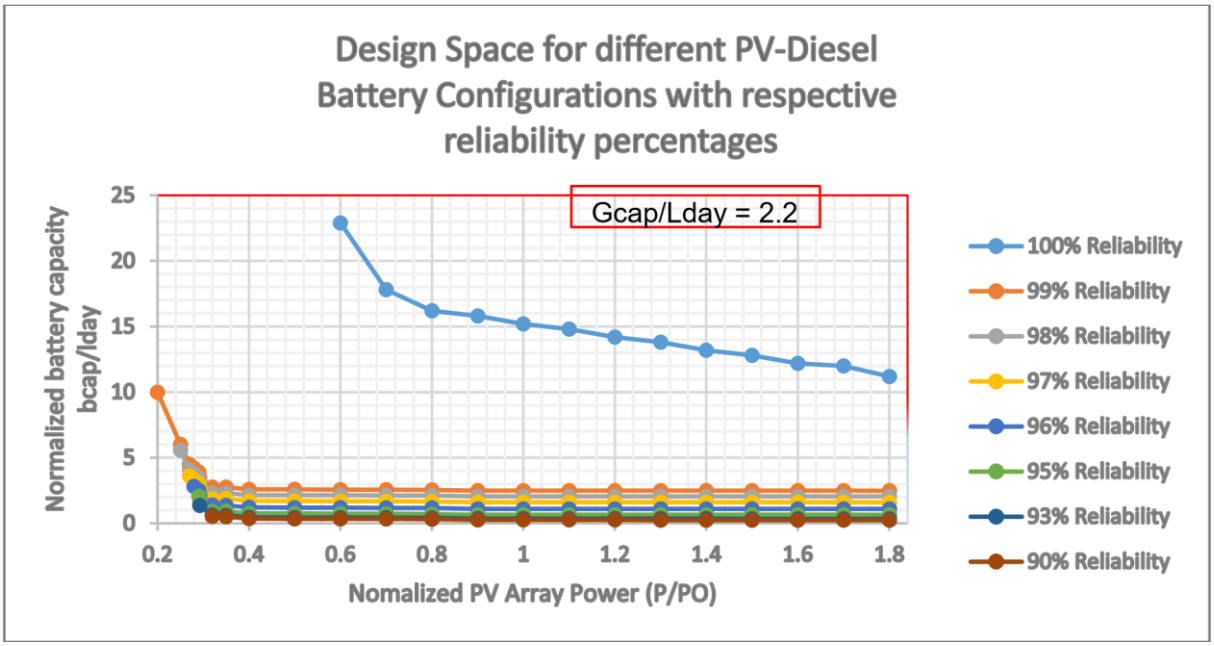

Figure 32 Design Space for different PV-Diesel Battery configurations with respective reliability percentages

Based on all the possible combinations shown in Figures 19 a) to 19 e), further optimization was performed and the marginal return curves that represented all minimum costs for different reliability levels were obtained and are shown in Figure 20. The marginal curves were plotted on the same graph and the curve which appeared at the bottom on the graph was the “Gcap = 2.2” marginal-return curve, and it was chosen.

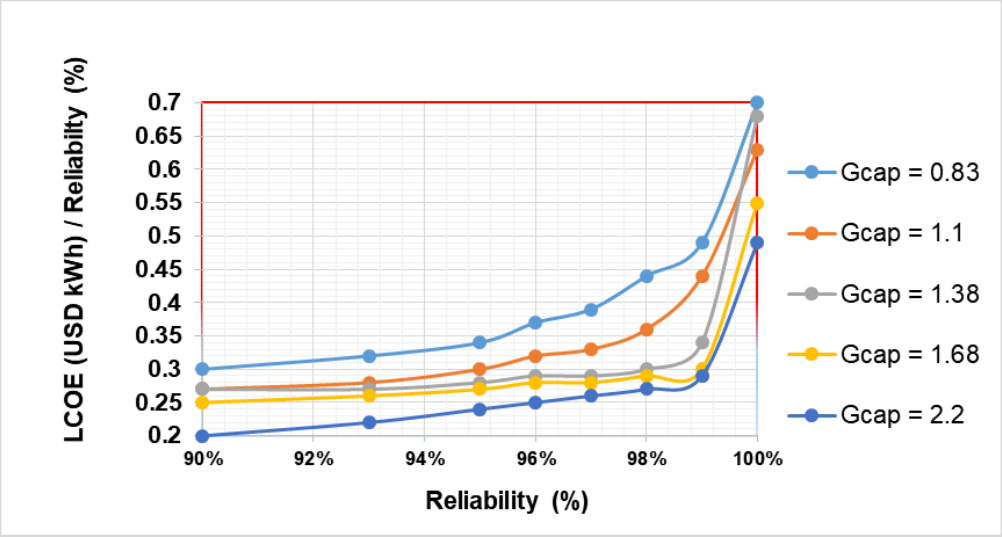

Figure 35 Marginal Return curves the selection of optimum design parameters (reliability)

Table 18 shows the dimensionless sizes for the battery bank, the PV array, and the generator required to achieve the desired 100% and 99% levels of reliability at the minimum LCOE of 0.49 USD/kWh and 0.29 USD/kWh respectively. The dimensionless sizes for the battery bank, the PV array, and the generator required to achieve the desired reliability of 100% and 99% at minimum LCOE were chosen from the "elbow" values shown in Figure 21.

Table 18 System Design Parameters for 100% and 99 % Reliability PV System

Reliability	USD/kW	GCap / Lday	P/Po	Bcap/ Lday
100%	0.49	2.2	16.2	0.8
99%	0.29	2.2	3.9	0.29

The graph shown in Figure 21, acted as a decision ground for deciding which system combination would offer the most benefits at the least cost. The graph shows that as reliability increases from 90% to 99%, the LCOE does not increase by much. Therefore, it was concluded that 99% reliability would offer the most benefits at the

least cost. However, increasing the reliability from 99% to 100% would increase the cost excessively.

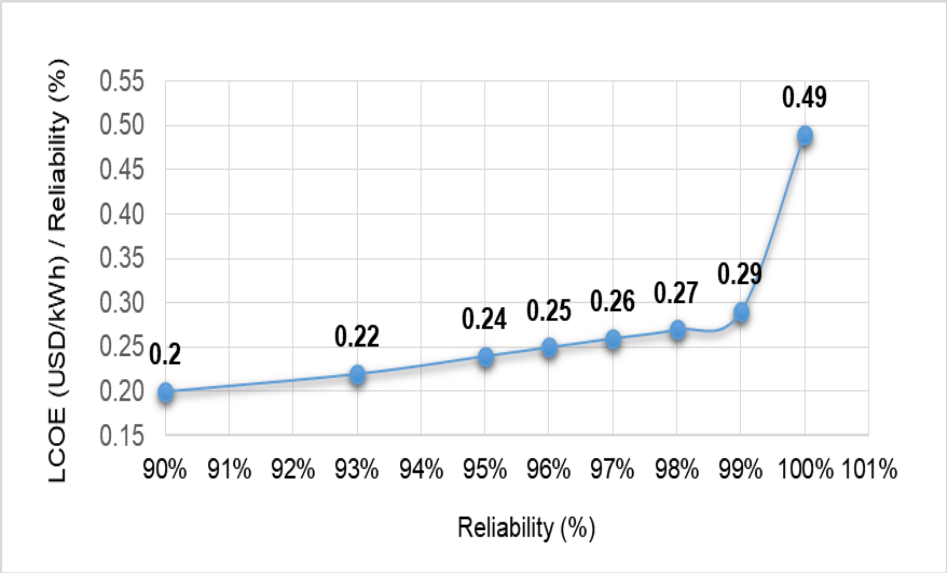

Figure 38 Marginal Return curve the selection of optimum design parameters (reliability)

As mentioned previously, the graph also confirmed that the system with 99% reliability would cost almost half of that of the system with 100% reliability. This indicated that it might not be justified to pay that much for the 1% increase in reliability. In terms of cost, the 1% increase could cost about the same as developing another system of the same capacity for another community. The amount that could thus be paid for the 1% increase in system reliability could also be used for providing other services to the community, such as water. Figure 22 a) indicates that for the dimensionless variable's curve ("Gcap = 2.2"), the PV variable was 22 while the battery's variable was 0.6, b) shows that for the curve ("Gcap = 2.2"), the PV variable was 10 while the battery's variable was 0.6. This confirmed that the cost of the 100%-reliability system would be approximately twice the cost of the 99%-reliability system. Out of the 8760 hours of the year, 1% amounted to approximately 88 hours which would be equivalent to 4 days. Losing 4 days of supply might be considered to be insignificant to the people living in the rural areas, who were used to living without any electricity. It might be argued that having energy that provides 99% reliability "would be more than perfect", as they did not own equipment that might require a 100%-reliable system.

a)

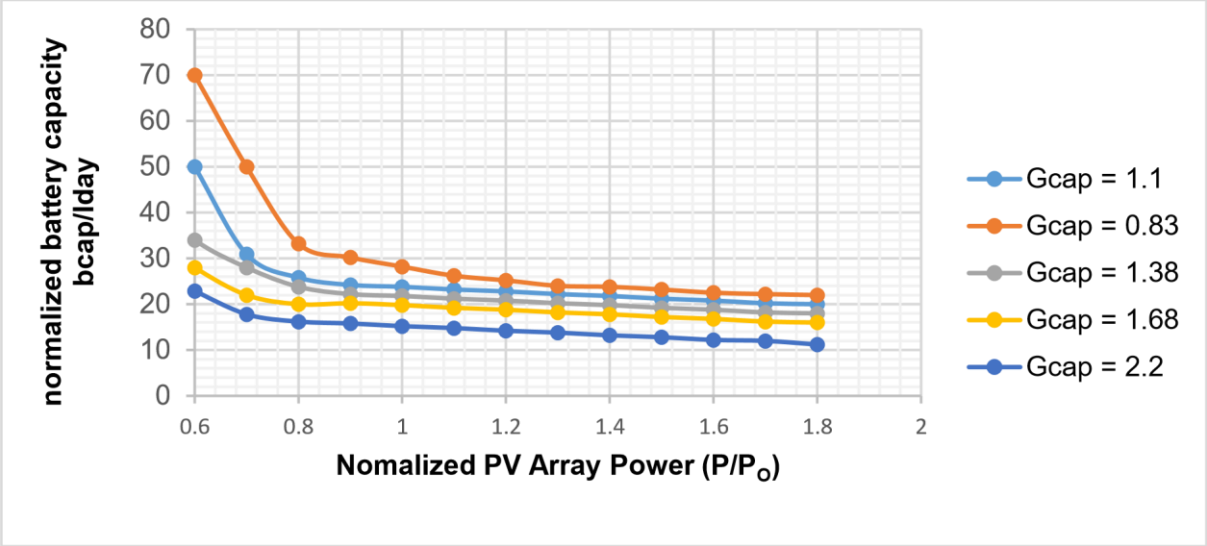

b)

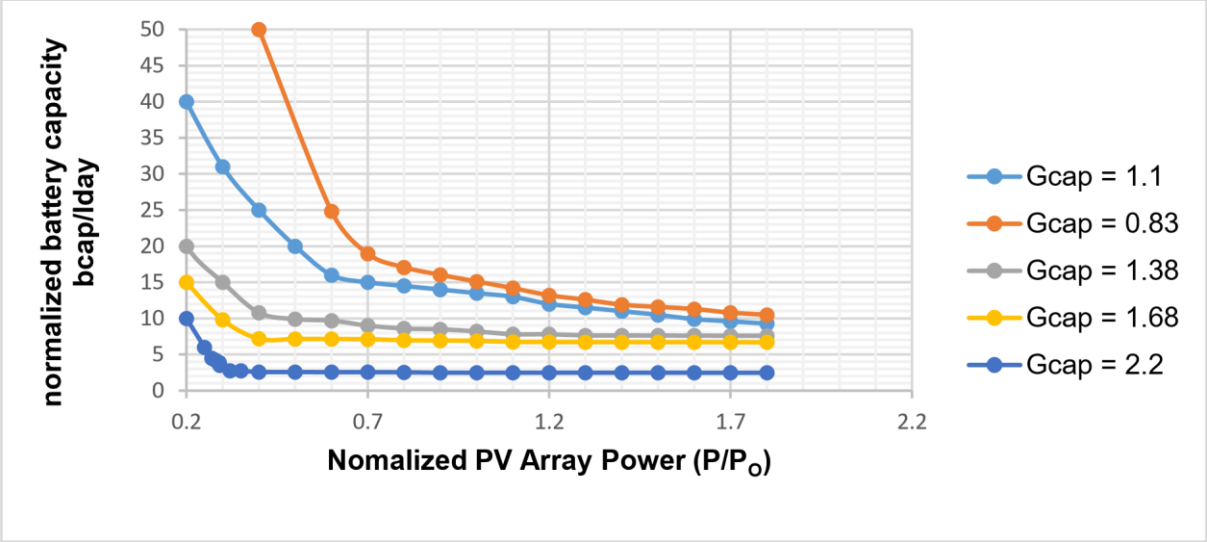

Figure 43 Sizing curves for a PV-Diesel-Battery Hybrid system for a) 100% reliability b) 99 % reliability

The system performing at minimal Levelized Cost of Energy (LCOE), would require dimensionless components with sizes of 2.2, 3.9, and 0.29 for the generator, the PV, and the battery, respectively. Using the reliability-cost approach, a system combination that would operate at the minimum cost and at the desired reliability, was found. The selected configuration was a combination of different technologies, and it would therefore be important to manage them correctly individually to maximize the

performance and to decrease costs further. The next section discuss the Energy Management System.

Comparison of our findings to the findings of Cicilio et al [52], reveals that both studies show slightly different values for the levelized cost of energy, generator size solar PV size and battery size as shown by Table 19. Therefore, our results provide more comparable results among different studies.

Table 19 Comparison of Ha Makebe and Ribaneng Inputs and outputs

	Cicilio et al (Ha Makebe)	This study (Ribaneng)
Number of Houses	212.00	250.00
Village peak Load	37.4 kW	56.6 kW
Battery size	215 kWh	255 kWh
Solar PV size	100 kW	115 Kw
Generator size	45 kW	40 kW
Levelized cost of energy	0.35 $/kWh	0.29 $/kWh

4.7 System Performance Simulations

For the simulation of the management of the resultant energy performance parameters for a 99%-reliability system, it two opposing days were selected: one being an overcast, cloudy day, and the other, a clear sunny day. The results of the simulation are shown in Figure 23 and Figure 24 respectively. Figure 23 shows that the selected site received partial solar radiation during day, and, as a result, there was an energy deficit until the next day. Most of the energy was produced during the day from the solar PV system when solar irradiance was high and during the night the energy was produced by the battery storage, and diesel generator supplied energy when solar energy was low. Figure 24 shows that during the first day when there was not enough radiation, the backup diesel generator served the load and there was no energy deficit.

The generator charges the battery storage if there was excess during the supply.

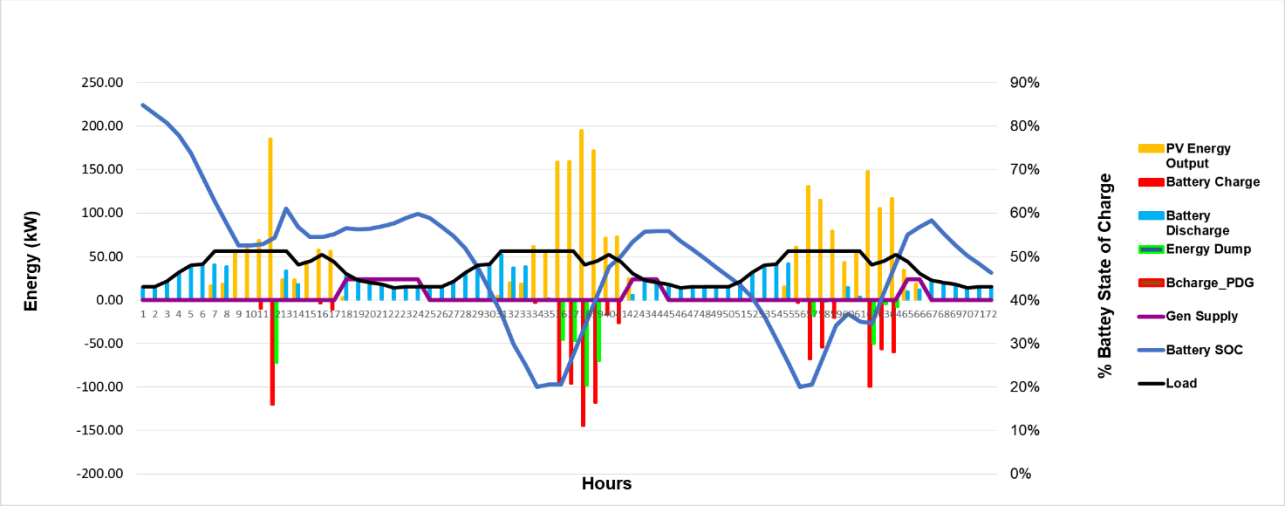

Figure 45 Graphic representation of PV-Battery system performance for 3 consecutive days selected (cloudy day)

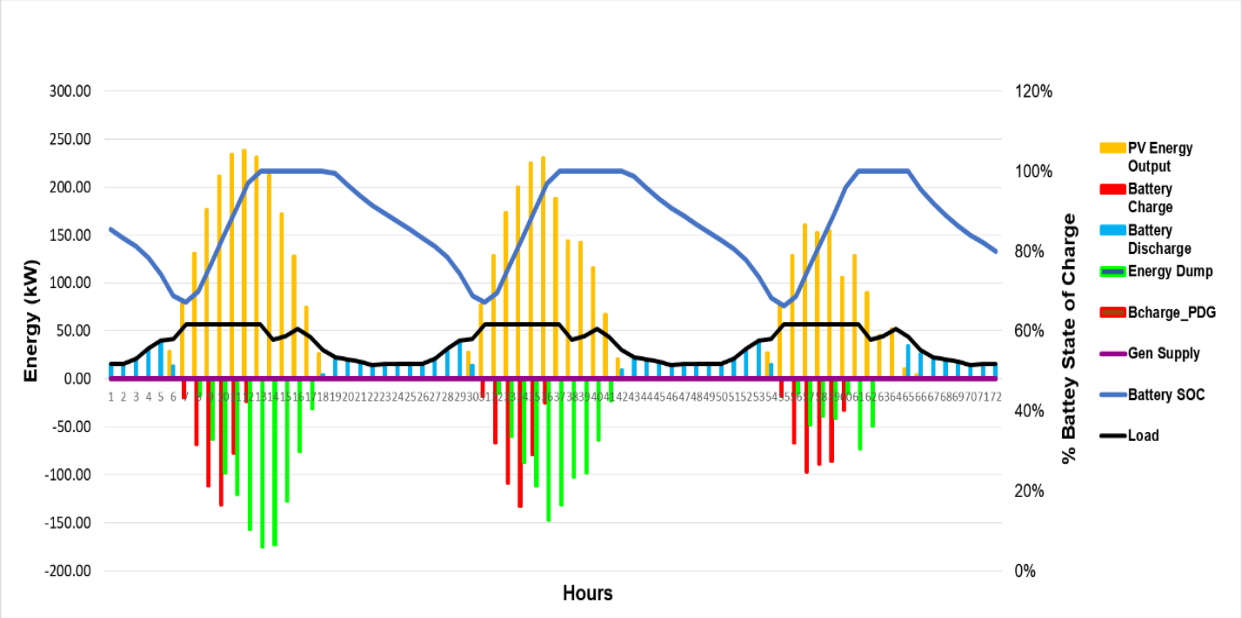

Figure 48 Graphic representation of PV-Diesel-Battery system performance for 3 consecutive days selected (clear sunny day)

4.8 Sensitivity analysis results

Results indicated that the changes in capital cost had significant effects on the LCOE. For example, a 20% decrease in capital cost reduced the LCOE by 13%, a further reduction in capital cost decreased the LCOE by 25% from the base case scenario. The variation of discount rate had also considerable effects on the LCOE for both PVDiesel-Battery and PV-Battery. The Battery cost had a huge effect on the PV-DieselBattery system more than it

has on the PV-Battery system. Results from this analysis also indicated that the fuel, PV module cost, and battery costs have insignificant effects on the LCOE hybridized systems.

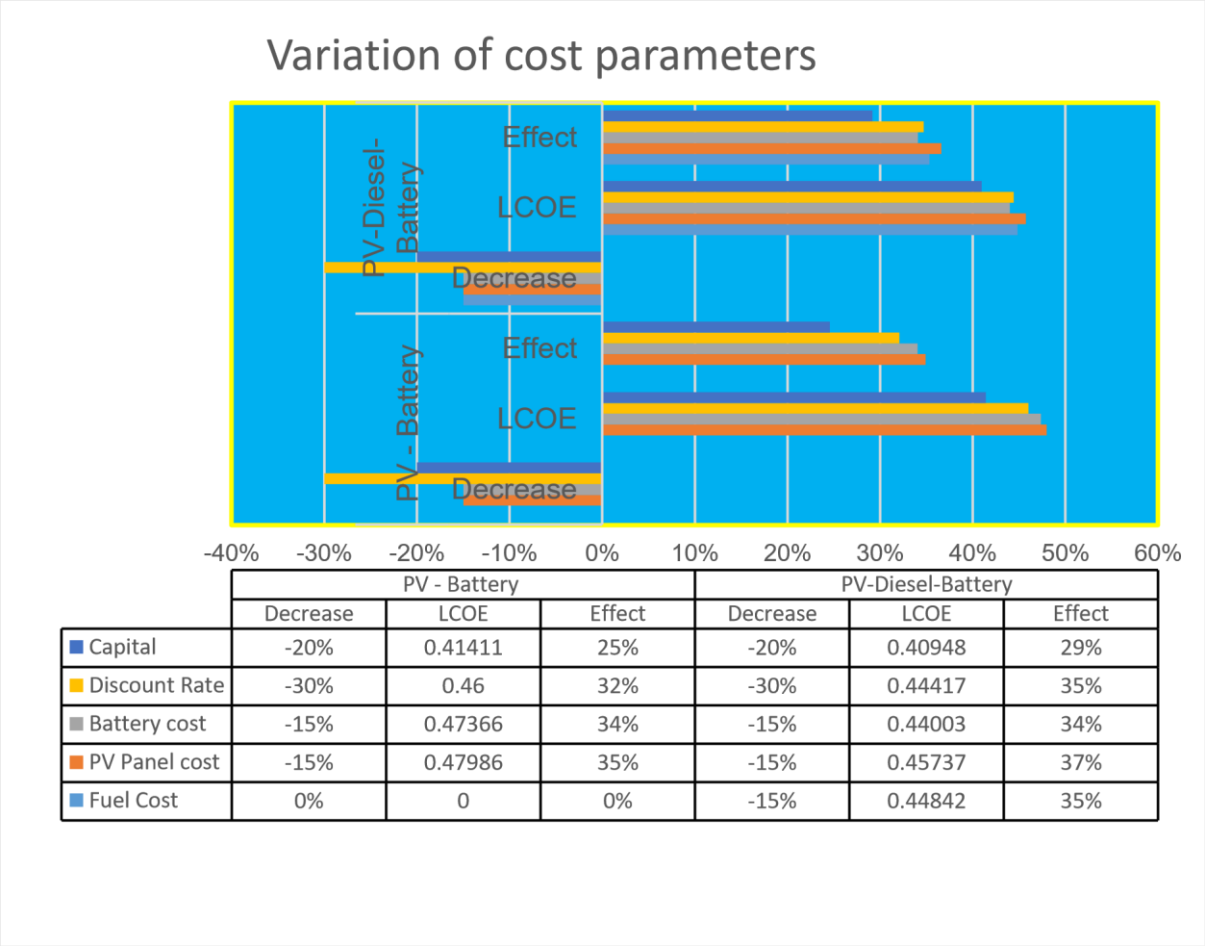

	PV - Battery			PV-Diesel-Battery		
	Decrease	LCOE	Effect	Decrease	LCOE	Effect
Capital	-20%	0.41411	25%	-20%	0.40948	29%
Discount Rate	-30%	0.46	32%	-30%	0.44417	35%
Battery cost	-15%	0.47366	34%	-15%	0.44003	34%
PV Panel cost	-15%	0.47986	35%	-15%	0.45737	37%
Fuel Cost	0%	0	0%	-15%	0.44842	35%

Figure 25 Effects of variation of input cost parameters on LCOE ($/kWh)

Chapter 5: Conclusions and Recommendations

5.1 Conclusions

The results produced by this study emphasized that different geographic locations have different renewable energy resources, which are also subject to different costs for setting up renewable energy plants, and these could produce electricity at different levels of energy-supply reliability. Therefore, modelling the energy flow in a photovoltaic-based off-grid power system comprising a PV array, a battery bank, and an auxiliary generator and the associated power conditioning equipment, made it possible to size an off-grid power system to achieve the desired energy-supply reliability at the least anticipated cost. Through a life-cycle cost analysis, the anticipated levelized cost of energy from the designed power system was determined,

to find a superior solution to overcome the obstacle encountered, i.e. the high investment costs involved with the generation of electricity from renewable energy sources. This solution would also support the endeavours to attract investments in the use of RE in Lesotho.

The system was designed to incorporate the best technology available while adhering to the least cost constraint, by using a dimensioning approach that considered both the power-supply reliability and the Levelized Cost of Energy. Adopting the practice of engineering intuition and calculations, the 99%-reliability level was recommended as the specified required reliability level that would meet the least-cost-of-power generation constraint. Policymakers may, however, argue that depending on the load shape, load behavior, future additional loads, climatic conditions, political and economic issues, other levels of reliability could be favored.

In summary, the findings of this study are: the proposed system for Riabaneng in the district of Mohale's Hoek, Lesotho, is an optimized PV mini-grid system which would operate a 99%-reliability level at the least Levelized Cost of Energy of 0.29 USD/kWh, with an average daily energy demand of 879.23 kWh/day for the community. The total projected annualized energy demand was predicted to be about 320.9 MWh/year. The PV mini-grid system proposed would need capacities of 140 kW and 4.5 kW for the solar inverter and charger inverter respectively, a PV array with a capacity of 140 kWp with 255 kWh of battery capacity at an estimated capital investment cost of $ 383,161.

It was found that, we could develop systems that were sufficiently reliable but with much lower cost than the 100% reliability systems. Therefore it was not worth going for 100% reliability systems. It was also established that people could live with the 1% loss of load very well. Cost was one inhibiting factor, however the study could reduce the cost of PV systems by halve, which was significant as more people might begin to take the technology. The aim of the study was to see more people to be able to afford the technology.

5.2 Recommendations

The following recommendations are made:

- The government together with civil and private societies should recognized the need for more awareness on PV mini- grid systems and their optimum design at the least levelized cost of energy.

- Training institutions should be resourced and encouraged to train local experts on the design installation, operations and maintenance of PV mini-grid systems.

- Energy Stakeholders and the Private and Civil society should be encouraged to implement solar PV mini-grid systems as it has proven to be a viable complement to national grid extension in the fight against energy poverty.

Different dispatch strategies have not been analyzed extensively in this study. Additionally, using different batteries have not received much attention. Therefore further work that should be done is to investigate the effects of different dispatch strategies and on the Cost of Energy (COE) and the Net Present Cost (NPC) and the study should further be extended to analyze the effects of battery technologies on the COE, NPC, and the consequential indicators. However, environmental emissions are significantly affected with dispatch strategies, therefore should also be investigated deeply.

References

[1] A. Lewandowska-Bernat and U. Desideri, 'Sustainable mini-grid', *Energy Procedia*, vol. 142, pp. 3008–3013, Dec. 2017, doi: 10.1016/j.egypro.2017.12.437.

[2] M. Moner-Girona, E. Ackom K., M. Solano-Peralta, X. Vallve, M. Lazopoulou, and S. Szabo, 'Electrification of Sub-Saharan Africa through PV/hybrid mini-grids: Reducing the gap between current business models and on-site experience', *Renewable and Sustainable Energy Reviews*, vol. 91, pp. 1148–1161, 2018.

[3] Department of Energy, 'Lesotho SEforAll Country Investment Prospectus', Ministry of Energy and Meteorology, Maseru, Lesotho, 2018. Accessed: Nov. 20, 2018. [Online].

[4] D. Fernandez and R. Tobich, 'FORMULATION OF THE LESOTHO ELECTRICATION MASTER PLAN', AETS Consortium, Maseru, Lesotho, Analytical Report CRIS 2017/387289/1, 2018. Accessed: Mar. 09, 2019. [Online]. Available: https://erc.nul.ls/publications/reports.

[5] T. Hadjicostas and D. Padayachy, 'FORMULATION OF THE LESOTHO ELECTRICATION MASTER PLAN'. AETS Consortium, 2017, Accessed: Mar. 16, 2019. [Online]. Available: https://erc.nul.ls/publications/reports.

[6] D. Fernandez and R. Tobich, 'Formulation of the Lesotho Electrification master Plan: Off-Grid Master Plan Report', European Union, Maseru, Lesotho, Final Report CRIS 2017/387289/1, 2014. Accessed: Jul. 13, 2019. [Online].

[7] R. Deshmukh, J. P. Carvallo, and A. Gambhir, 'Sustainable Development of Renewable Energy Mini-grids for Energy Access'. University of California, Mar. 2013, Accessed: Mar. 05, 2017. [Online].

[8] C. Miller, C. Altamirano-Allede, N. Irshad, and S. Biswas, 'POVERTY ERADICATION THROUGH ENERGY INNOVATION', AZU. Aizona State University, AZ.Arizona, Funtional Report Feb 2018, Feb. 2018. Accessed: Mar. 08, 2019. [Online].

[9] IEA-ETSAP and IRENA, 'Renewable Energy Integration in Power Grids - Technology Brief E15'. International Renewable Energy Agency, 2015, Accessed: Jun. 02, 2019. [Online]. Available: www.etsap.org – www.irena.org.

[10] UNDP, 'UNDP | Procurement Notices - 55547 - FINANCIAL SUPPORT SCHEME', *United Nations Capital Development Fund*, May 30, 2019. http://procurement-notices.undp.org/view_notice.cfm?notice_id=55547 (accessed May 30, 2019).

[11] AF. Mercados EMI, 'Regulatory Framework for the Development of Renewable Energy Resources in Lesotho', Lesotho Electricity and Water Authority, Maseru, Lesotho, Final Report MI 1582, 2015. Accessed: May 25, 2019. [Online].

[12] DOE, 'Lesotho Renewable Policy 2015-2025'. Ministry of Energy, 2015, Accessed: Oct. 30, 2018. [Online].

[13] RAPS Consulting, 'Lesotho Energy Access Strategy Project', GTZ-EUEI/PDF, Lesotho, Baseline Study report 83001486, 2007. Accessed: Aug. 02, 2019. [Online].

[14] SSI A DHV COMPANY, 'Lesotho Power Generation: Solar Power Generation Option-Volume 1 Part 1.3', LEC.Lesotho Electricity Company (Pty) Ltd, Msu, Lesotho, Final Milestone LEC/GEN/1-2009, 2009. Accessed: Mar. 08, 2019. [Online]. Available: https://erc.nul.ls/publications/reports.

[15] Atkins, 'Renewable Energy and Energy Efficiency Strategy & Action Plan', EU SEA4ALL.Sustainable Energy For ALL, SADC. Southern Africa, Periodic REEESAP 2016-2030, Oct. 2016. Accessed: Oct. 30, 2018. [Online].

[16] SolarGIS, 'PV electricity and solar radiation', *Global Solar Atlas*, Oct. 23, 2019. https://globalsolaratlas.info/map?c=-28.381735,27.004395,7&s=28.497661,28.377686&m=site (accessed Oct. 23, 2019).

[17] SEforALL Africa Hub, 'Lesotho Rapid Assessment and Gap Analysis', SEforALL.Sustainable Energy For All, Msu, Lesotho, Analytical Report 1, 2001. Accessed: Mar. 17, 2019. [Online].

[18] S. Tayyab, 'Business models for mini-grids', Smart Villages Initiative, Malaysia, Technical Report 9, 2017.

[19] M. Oliveira, 'OPPORTUNITIES AND CHALLENGES IN THE MINI-GRID SECTOR IN AFRICA'. EEP Africa, 2018, Accessed: Mar. 08, 2019. [Online]. Available: https://erc.nul.ls/publications/reports.

[20] DOE, ‘Lesotho Energy Policy 2015-2025’. Ministry of Energy and Meteorology, 2015, Accessed: Mar. 05, 2019. [Online]. Available: https://erc.nul.ls/publications/reports.
[21] SEforALL Africa Hub, African Bank, Carbon Trust, Sustainable energy fund Africa, UNEP, and ECREEE, ‘Green Mini Grid Market Development Programme’, AB.African Bank, MZ.Mozambique, Periodic Report 5, Apr. 2017. Accessed: Mar. 08, 2019. [Online].
[22] O. Drücke, ‘Village electrification in Africa using PV Mini-Grids: A case study from Senegal’, in *POWER THE WAY TO SUSTAINABILITY*, Senegal, Jul. 2015, vol. 1–21.
[23] M. Wiemann, S. Rolland, and Glania, ‘HYBRID MINI-GRIDS FOR RURAL ELECTRIFICATION: LESSONS LEARNED’. Alliance for Rural Electrification (ARE), 2011.
[24] C. Blodgett, P. Dauenhauer, H. Louie, and L. Kickham, ‘Accuracy of energy-use surveys in predicting rural mini-grid user consumption’, *Energy for Sustainable Development*, vol. 41, pp. 88–105, Dec. 2017, doi: 10.1016/j.esd.2017.08.002.
[25] ESMAP, ‘Technical and Economic Assessment of Off-grid, Mini-grid and Grid Electrification Technologies’. THE WORLD BANK, 2007.
[26] M. J. Saulo and V. O. Omondi, ‘Design and Analysis of Solar Energy Mini-Grid for Rural Electrification’, *OALib*, vol. 02, no. 09, pp. 1–10, 2015, doi: 10.4236/oalib.1101903.
[27] R. AbdelHady, ‘Modeling and simulation of a micro grid-connected solar PV system’, *Water Science*, vol. 31, no. 1, pp. 1–10, Apr. 2017, doi: 10.1016/j.wsj.2017.04.001.
[28] J. Khoury, R. Mbayed, G. Salloum, and E. Monmasson, ‘Optimal sizing of a residential PV-battery backup for an intermittent primary energy source under realistic constraints’, *Energy and Buildings*, vol. 105, pp. 206–216, Oct. 2015, doi: 10.1016/j.enbuild.2015.07.045.
[29] T. Hove, ‘A method for predicting long-term average performance of photovoltaic systems’, *Renewable Energy*, vol. 21, no. 4, pp. 207–229, 2000.
[30] T. Hove and H. Tazvinga, ‘A techno-economic model for optimising component sizing and energy dispatch strategy for PV-diesel-battery hybrid power systems’, *Journal of Energy in Southern Africa*, vol. 23, no. 4, pp. 18–28, 2012.
[31] X. Pons and M. Ninyerola, ‘Mapping a topographic global solar radiation model implemented in a GIS and refined with ground data’, *Int.J.Climatol*, vol. 28, pp. 1821–1834, 2008.
[32] T. Cebecaucer, A. Skoczek, and M. Suri, ‘The effect of solar radiation data types on calculation of tilted and suntracking solar radiation’, in *Solar Energy*, Hamburg Germany, 2011, pp. 1–6.
[33] ESRA, *European Solar Radiation Atlas*, 4th ed. Paris, France: Presses de l’Ecole des Mines de Paris, 2000.
[34] M. Suri, T. Huld, T. Cebecaucer, and E. Dunlop, ‘Geographic Aspects of Photovoltaics in Europe: Contribution of the PVGIS Web Site’, *IEEE Journal of Selected Topics in Applied Earth Observations and Remote Sensing*, vol. 1, pp. 34–41, 2008.
[35] RETScreen, ‘Clean Energy Project Analysis Software’, *RETScreen*, 2019. http://www.retscreen.net/.

[36] R. Aguiar and M. Collares-Pereira, ‘A time dependent, autoregressive, Gaussian model for generating synthetic hourly radiation’, *Solar Energy*, vol. 49, pp. 167–174, 1992.
[37] M. Gunther, ‘Advanced CSP Teaching Materials Chapter 2 Solar Radiation - Semantic Scholar’, *Simanticscholar*, 2011. https://www.semanticscholar.org/paper/Advanced-CSP-Teaching-Materials-Chapter-2-Solar-G%C3%BCnther-Janotte/2017ec3c150ba4427561ace2b8273484f3b907c8 (accessed Oct. 22, 2019).
[38] S. A. Kalogirou, *Solar Energy Engineering: Processes and Systems*, 2nd ed. London: Elsevier, 2014.
[39] A. A. M. Sayigh, *Solar Energy Engineering*, 1st ed. Newyork: Academic Press, 1977.
[40] J. A. Duffie and W. A. Beckman, *Solar Engineering of Thermal processes*, 4th ed. Canada: John Wiley & Sons, Ltd, 2013.
[41] M. Iqbal, *AN INTRODUCTION TO SOLAR RADIATION*, 1st ed. Canada: Academic Press, 1983.
[42] RETScreen, *Clean Energy Project Analysis: RETScreen® Engineering & Cases TextbooK*, 3rd ed. Canada: Natural Resources Canada, 20005.
[43] D. Y. Goswami, *Principles of Solar Engineering*, 3rd ed. USA: CRC Press, 2015.
[44] IEA PVPS Task 11, ‘World-wide overview of design and simulation tools for hybrid PV systems’, IEA.International Energy Agency, Madrid, Spain, Technical Report Report IEA-PVPS T11-01, 20111.
[45] D. H. W. Li, S. W. Lou, and J. C. Lam, ‘An Analysis of Global, Direct and Diffuse Solar Radiation’, *In Energy Procedia*, vol. 75, pp. 388–393, 2015.
[46] C. Guemard, ‘Critical analysis and performance assessment of clear sky solar irradiance models using theoretical and measured data.’, *Solar Energy*, vol. 51, pp. 385–397, 1993.
[47] R. Kumar and I. Umanand, ‘Estimation of global radiation using clearness index model for sizing photovoltaic system.’, *Review Energy*, vol. 30, pp. 2221–2233, 2005.
[48] T. R. Ayotele and A. S. O. Ogunjuyigbe, ‘Prediction of monthly average global solar radiation based on statistical distribution of clearness index.’, *Energy*, vol. 90, pp. 1733–1742, 2015.
[49] J. F. Orgill and K. G. T. Hollands, ‘Correlation equation for hourly diffuse radiation on a horizontal surface.’, *Solar Energy*, vol. 19, pp. 357–359, 1977.
[50] A. Pedersen and Knight, ‘Solar Resource Mapping in Tanzania: Solar Modelling Report’, World Bank Group, Tanzania, Analytical Report ESMAP 96827, 2015.
[51] V. Taylor and L. Stowe, ‘Reflectance characteristics of uniform earth and cloud surfaces derived from Nimbus 7 ERB’, *Journal of Geophysical Research*, vol. 89, pp. 4987–4996, 1984.
[52] P. Cicilia, M. Orosz, A. Mueller, and E. Cotilla-Sanchz, ‘uGrid: Reliable Minigrid Design and Planning Toolset for Rural Electrification’, *IEEE Access*, vol. 7, pp. 1–12, 2019.
[53] G. Koucoi, D. Yamegueu, Q.-T. Tran, Y. Couliblay, and H. Buttin, ‘Energy

Management Strategies for Hybrid PV/Diesel Energy Systems: Simulation and Experimental Validation', *Energy and Power Engineering*, vol. 5, no. 1, pp. 6–14, 2016.

[54] C. Ghenai and M. Bettayeb, 'Modelling and performance analysis of a stand alone hybrid solar PV/Fuel Cell/Diesel Generator power system for university building', *Energy*, vol. EGY 14492, pp. 1–23, 2019.

[55] M. Jamshidi and A. Askarzadeh, 'Techno-economic analysis and size optimization of and off-grid hybrid photovoltaic, fuel cell and diesel generator system', *Sustainable Cities and Society*, vol. 44, pp. 310–320, 2019.

[56] D. Thevenard and A. Driesse, 'UNCERTAINTY IN LONG-TERM PHOTOVOLTAIC YIELD PREDICTIONS', Canada, Report 2010-122 (RP-TEC) 411-IEARES, 2010.

[57] A. Pueyo, S. Bawakyillenuo, and H. Osiolo, 'Cost and Returns of Renewable Energy in Sub-Saharan Africa: A Comparison of Kenya and Ghana', Uk, Evidence Report E190, 2016.

[58] NREL, 'Renewable Energy Cost Modeling: A Toolkit for Establishing Cost-Based Incentives in the United States.', Golden, Colorado, 2011, vol. 1, pp. 1–10.

[59] UNDP & ETH Zürich, 'Derisking Renewable Energy Investment: Off-Grid Electrification', ETH Zürich, Energy Politics Group, New York, 2018.

[60] C. Li, 'Techno-economic feasibility study of autonomous hybrid wind/PV/battery power system for a household in Urumqi, China.', *Energy*, vol. 55, pp. 263–272, 2013.